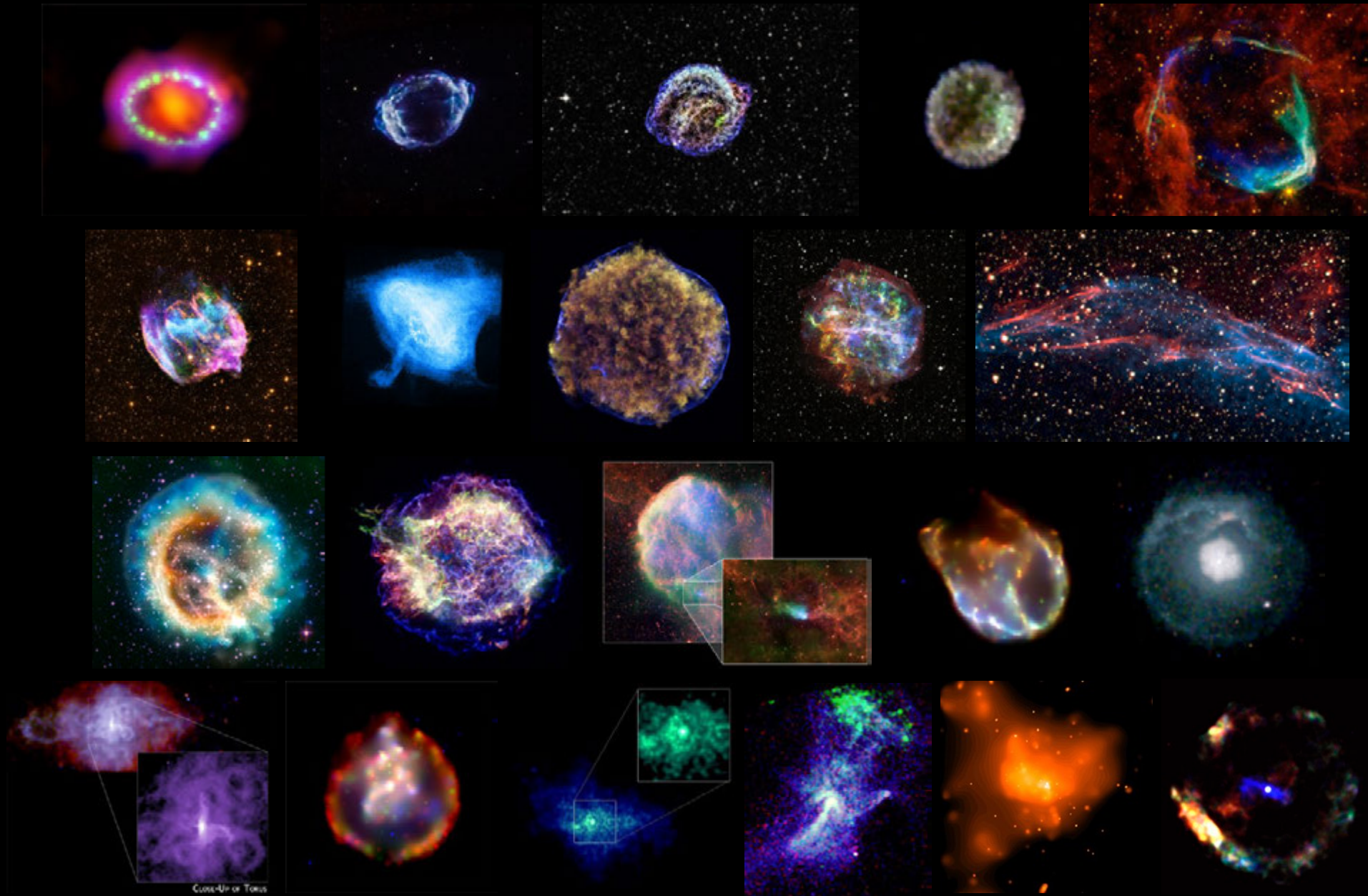


The Morphologies of Supernova Remnants



Laura A. Lopez
(The) Ohio State University
9 June 2019

Conclusions

Conclusions

SNR morphologies in different wavebands reflect the explosion asymmetries, the inhomogeneous environments, and the ambient magnetic field/particle acceleration properties

Conclusions

SNR morphologies in different wavebands reflect the explosion asymmetries, the inhomogeneous environments, and the ambient magnetic field/particle acceleration properties

Type Ia SNRs are more circular and symmetric in X-rays and IR, reflecting their distinct explosions & environments.

Conclusions

SNR morphologies in different wavebands reflect the explosion asymmetries, the inhomogeneous environments, and the ambient magnetic field/particle acceleration properties

Type Ia SNRs are more circular and symmetric in X-rays and IR, reflecting their distinct explosions & environments.

In radio, morphology reflects ambient density and B-field. Radio morphology becomes increasingly asymmetric with age due to expansion into inhomogeneous medium.

Conclusions

SNR morphologies in different wavebands reflect the explosion asymmetries, the inhomogeneous environments, and the ambient magnetic field/particle acceleration properties

Type Ia SNRs are more circular and symmetric in X-rays and IR, reflecting their distinct explosions & environments.

In radio, morphology reflects ambient density and B-field. Radio morphology becomes increasingly asymmetric with age due to expansion into inhomogeneous medium.

Distinct morphologies of different elements useful to constrain explosion/progenitors and origin of neutron star kicks

Conclusions

SNR morphologies in different wavebands reflect the explosion asymmetries, the inhomogeneous environments, and the ambient magnetic field/particle acceleration properties

Type Ia SNRs are more circular and symmetric in X-rays and IR, reflecting their distinct explosions & environments.

In radio, morphology reflects ambient density and B-field. Radio morphology becomes increasingly asymmetric with age due to expansion into inhomogeneous medium.

Distinct morphologies of different elements useful to constrain explosion/progenitors and origin of neutron star kicks

3D maps of SNRs are even more powerful at revealing asymmetries, microcalorimeters will revolutionize field

Morphological Classification



Shell-type
SNRs



Plerionic
SNRs



Composite
SNRs



Mixed-Morphology
SNRs

Morphological Classification



Shell-type
SNRs



Plerionic
SNRs



Composite
SNRs

Type Ia;
Core Collapse



Mixed-Morphology
SNRs

Tying SNRs to their Originating Explosions



Ways to classify explosions of SNRs
(Type Ia versus core-collapse):

- Identification of a central neutron star
- Light echoes (Rest et al. 2005, 2008; Krause et al. 2008)
- Metal abundance ratios (e.g., O/Fe)
- Environment (e.g., nearby molecular clouds)
- Nearby stellar populations
- Morphologies (Type Ia SNRs are more circular/symmetric than CC SNRs: Lopez et al. 2009, 2011; Peters et al. 2013)
- Fe line centroid (Type Ia SNRs have lower ionization state Fe than CC SNRs: Yamaguchi et al. 2014)

Tying SNRs to their Originating Explosions



Ways to classify explosions of SNRs
(Type Ia versus core-collapse):

- Identification of a central neutron star
- Light echoes (Rest et al. 2005, 2008; Krause et al. 2008)
- Metal abundance ratios (e.g., O/Fe)
- Environment (e.g., nearby molecular clouds)
- Nearby stellar populations
- Morphologies (Type Ia SNRs are more circular/symmetric than CC SNRs: Lopez et al. 2009, 2011; Peters et al. 2013)
- Fe line centroid (Type Ia SNRs have lower ionization state Fe than CC SNRs: Yamaguchi et al. 2014)

Using the Power-Ratio Method to Assess Morphology

Calculate multipole moments of the X-ray image (Buote & Tsai 1995, 1996; Jeltema et al. 2005)

Derived the same as in the expansion of 2D gravitational potential within a radius R (Binney & Tremaine, Section 2.4):

$$\Psi(R, \phi) = -2Ga_0 \ln \left(\frac{1}{R} \right) - 2G \sum_{m=1}^{\infty} \frac{1}{mR^m} (a_m \cos m\phi + b_m \sin m\phi)$$

$$a_m(R) = \int_{R' \leq R} \Sigma(\vec{x}') (R')^m \cos m\phi' d^2x'$$
$$b_m(R) = \int_{R' \leq R} \Sigma(\vec{x}') (R')^m \sin m\phi' d^2x'$$

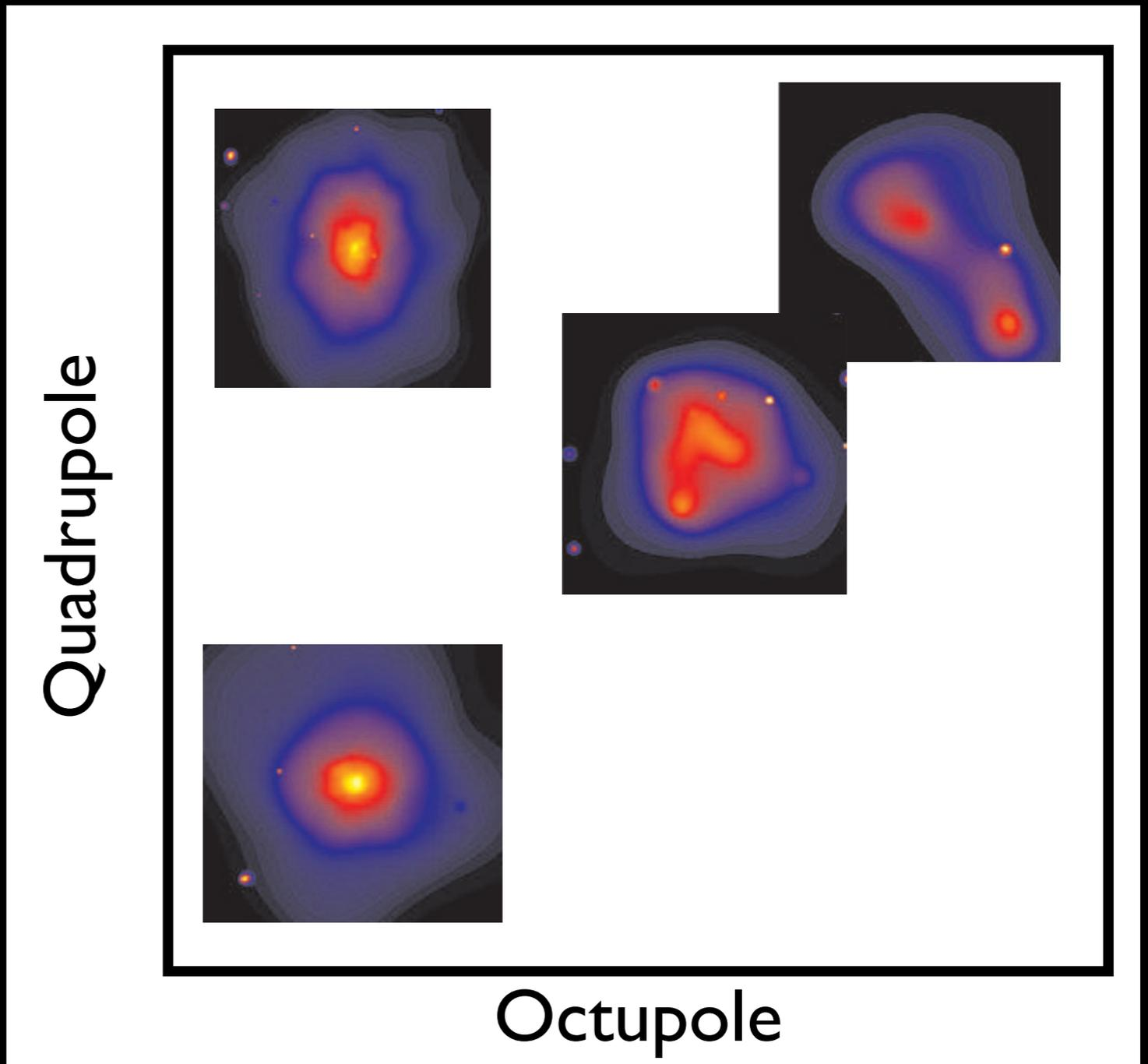
$\vec{x}' = (R', \phi')$ and Σ is the mass surface density (X-ray surface brightness in our calculation)

Using the Power-Ratio Method to Assess Morphology

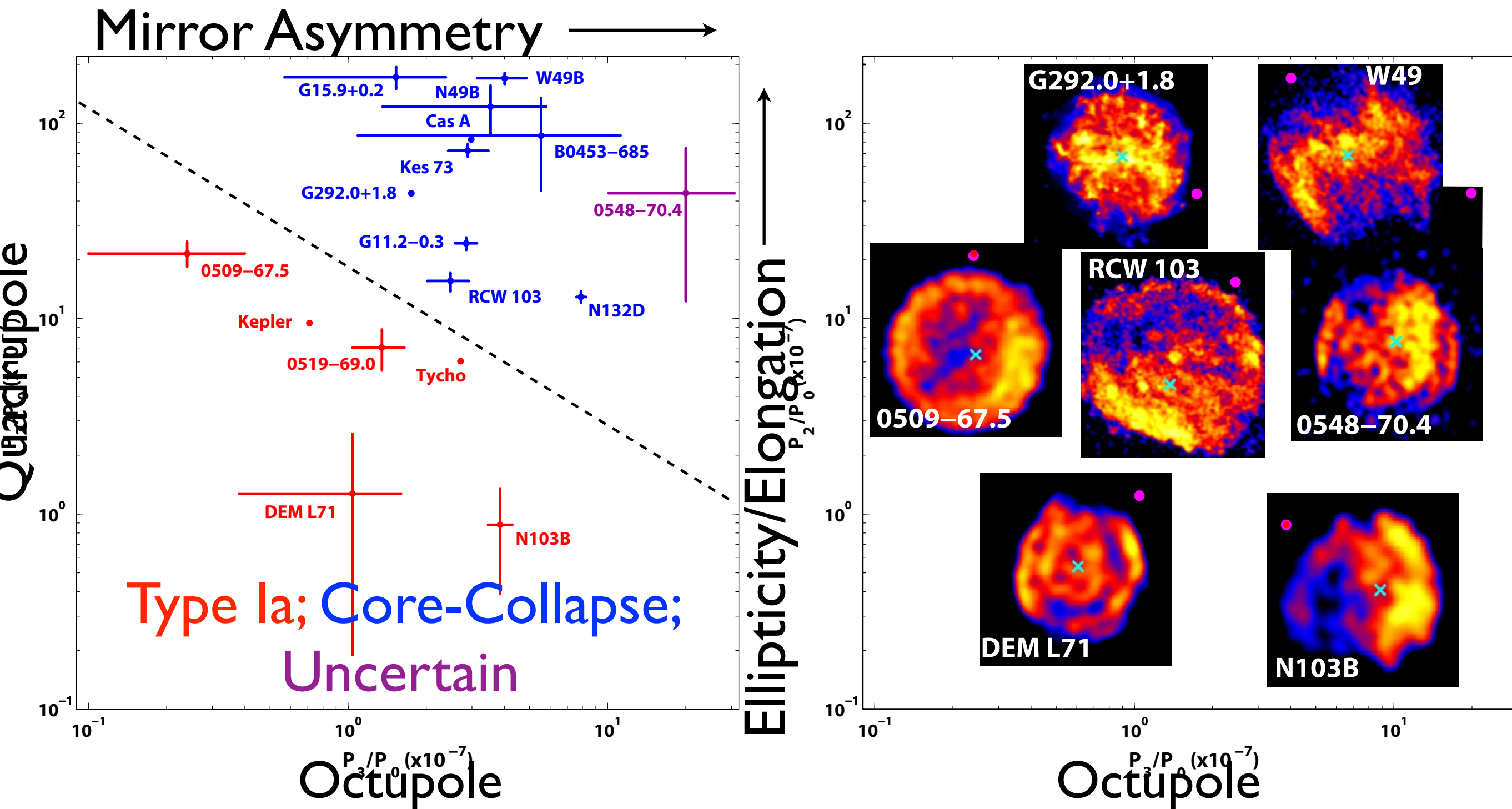
Calculate multipole moments of the X-ray image (Buote & Tsai 1995, 1996; Jeltema et al. 2005)

→ Quadrupole:
measure of ellipticity
Large for elliptical source,
small for circular source

→ Octupole:
measure of mirror
asymmetry
Large for sources with one
brighter side; small for
homogeneous sources



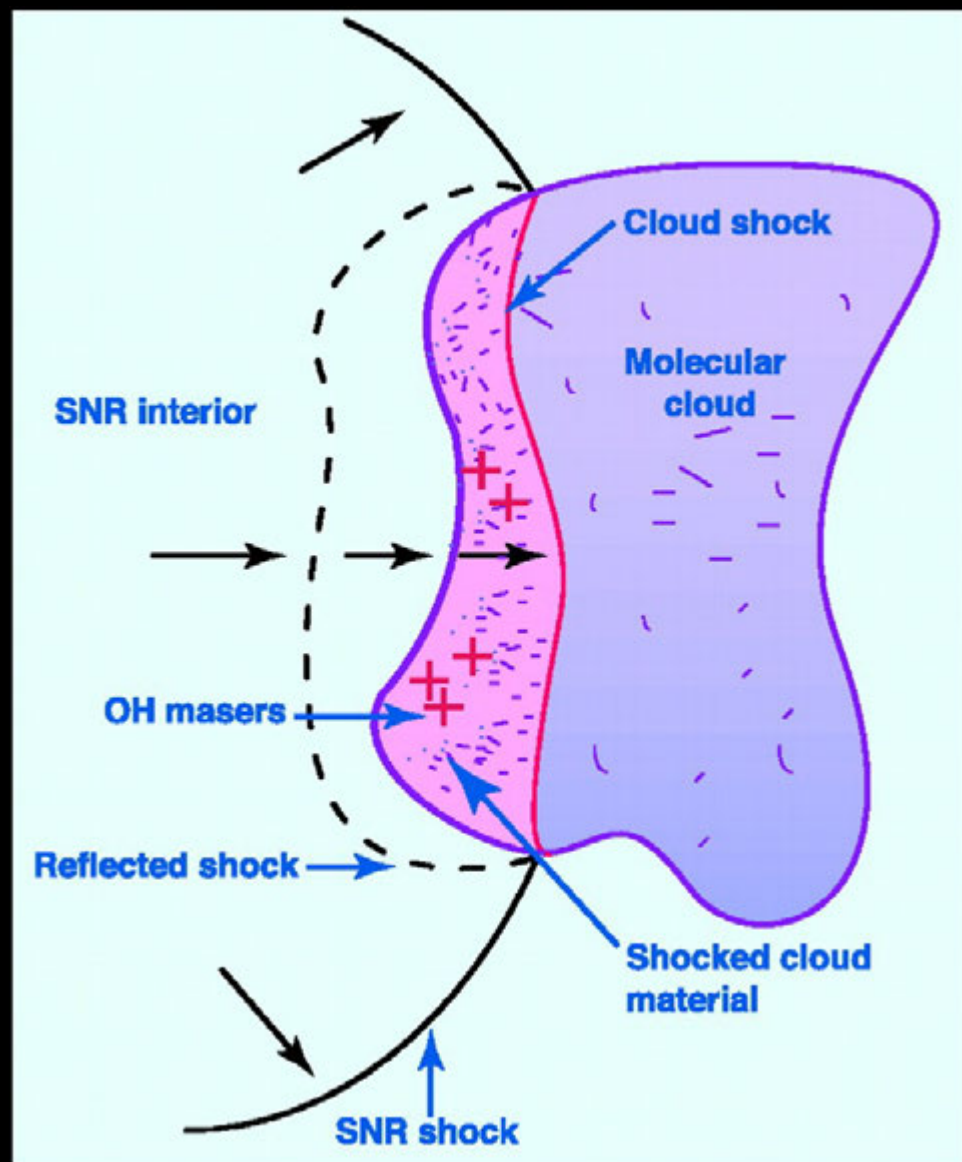
Morphology of Silicon Line Emission in X-rays



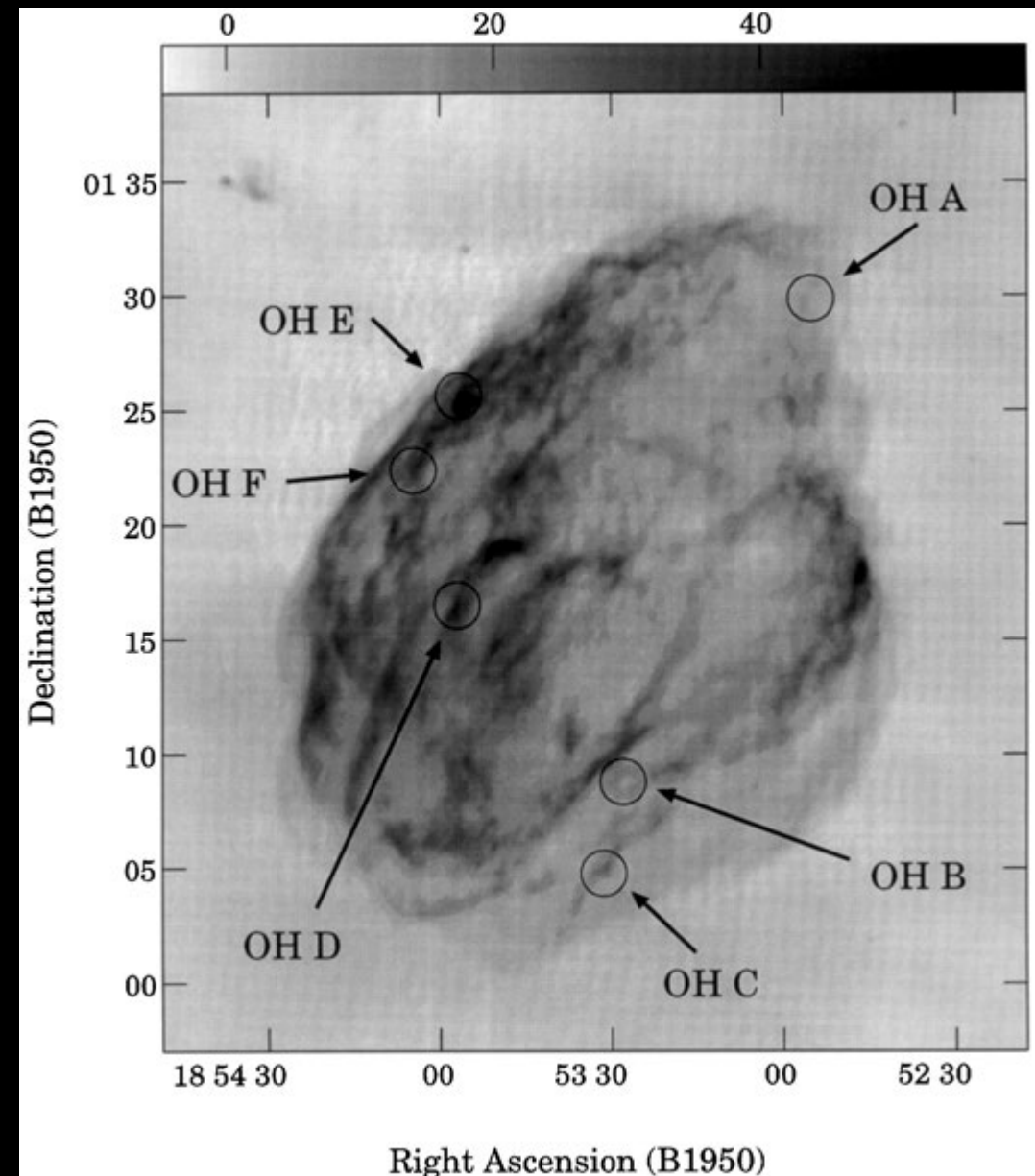
Environment Shapes Morphology

~70 / 300 supernova remnants show signs of interaction with molecular clouds (Jiang et al. 2010)

Signs of interaction: masers, CO or warm H₂, gamma-rays



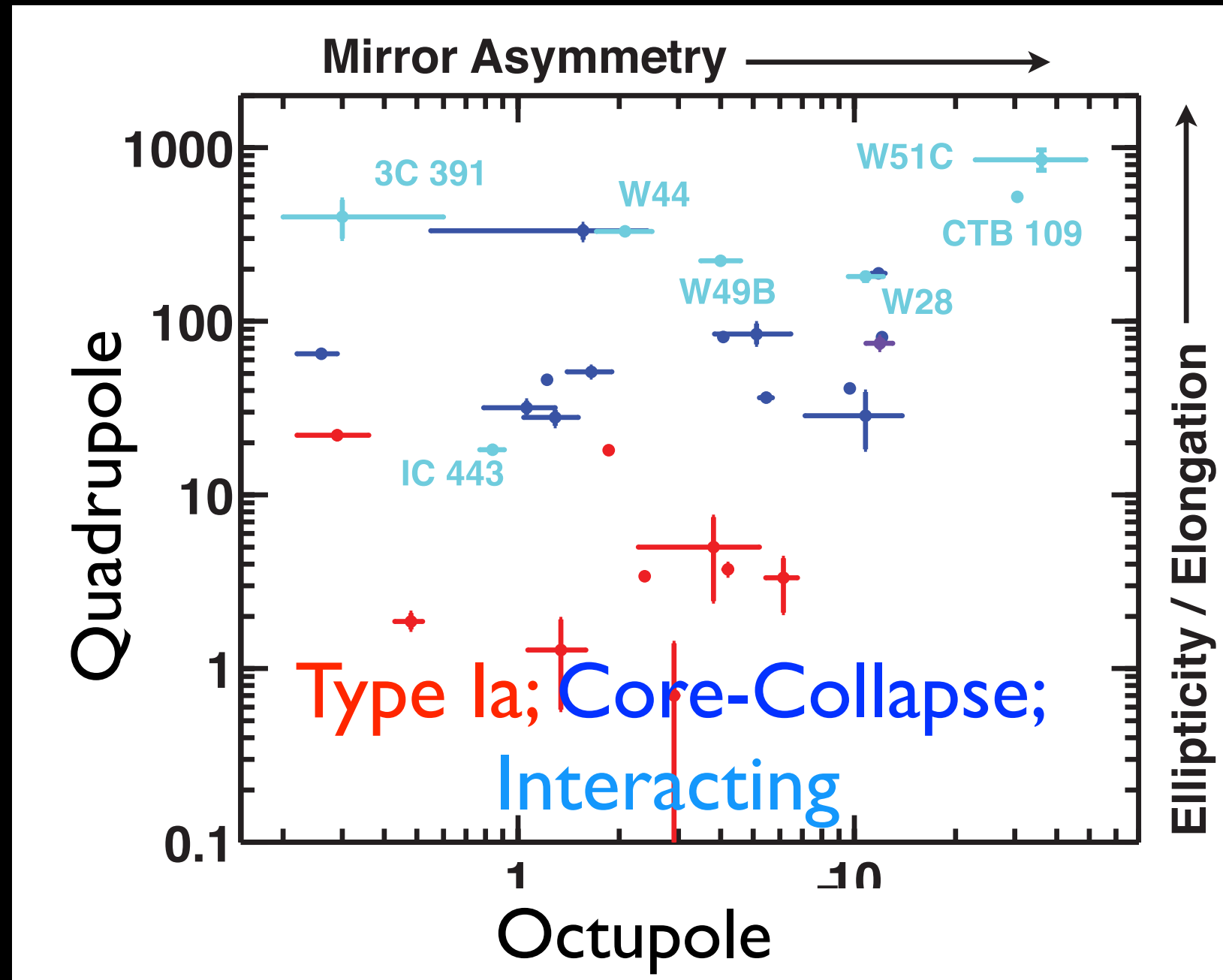
Wardle &
Yusef-Zadeh 2002



Claussen et al. 1997

Environment Shapes Morphology

SNRs interacting with molecular clouds tend to be the most elongated/elliptical (Lopez 2014; Holland-Ashford et al. 2017)



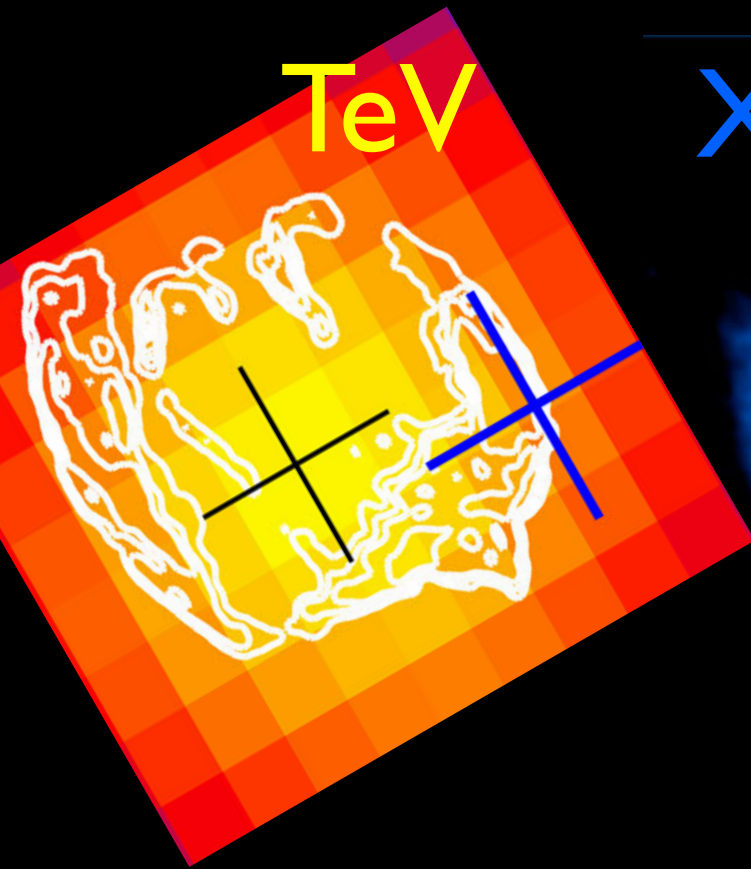
Lopez 2014

Other Wavebands?

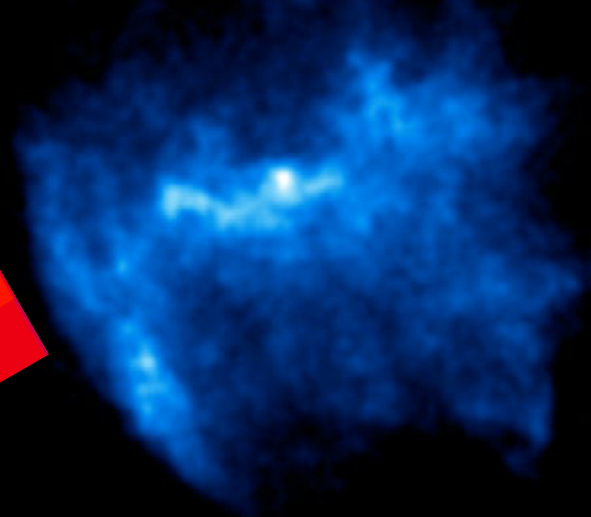
X-ray



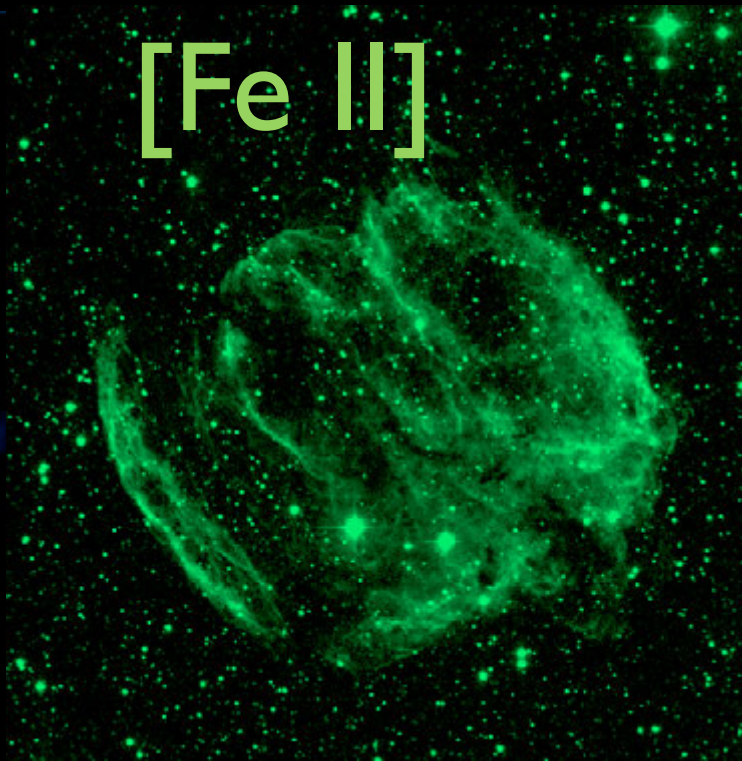
Other Wavebands?



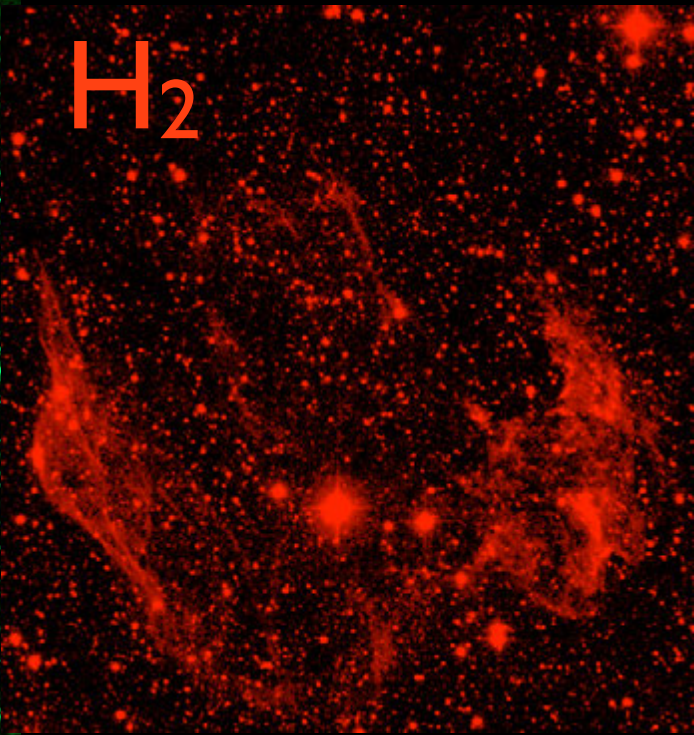
X-ray



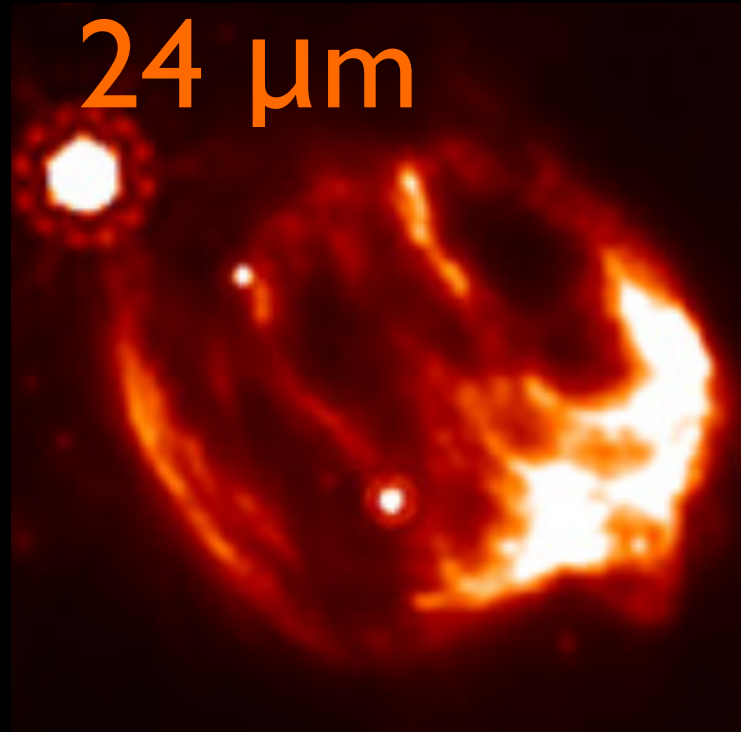
[Fe II]



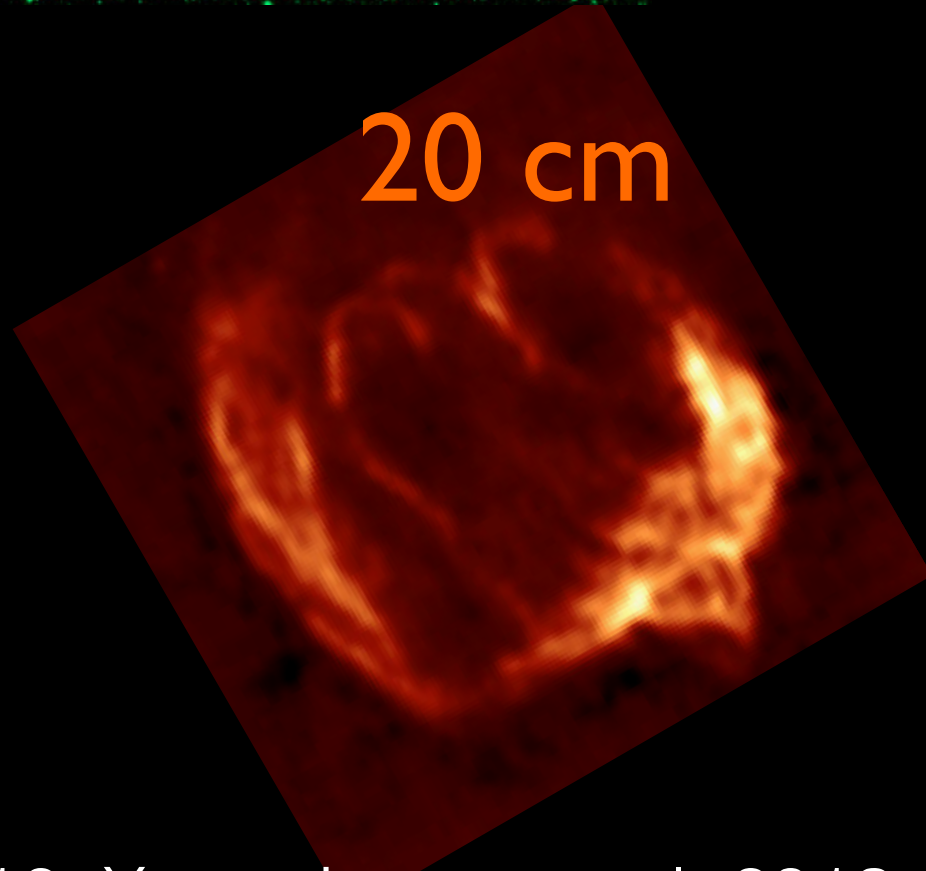
H₂



24 μm



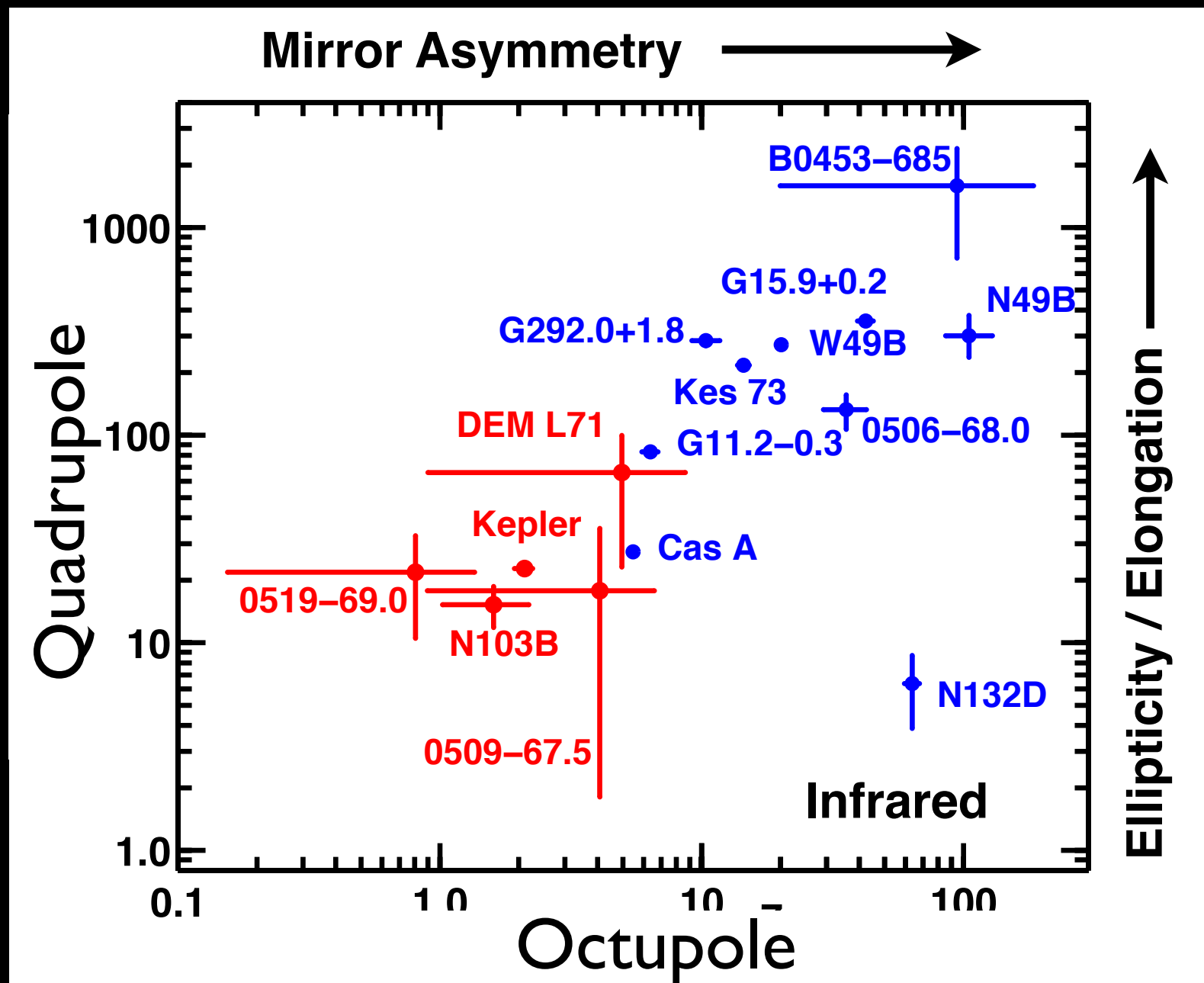
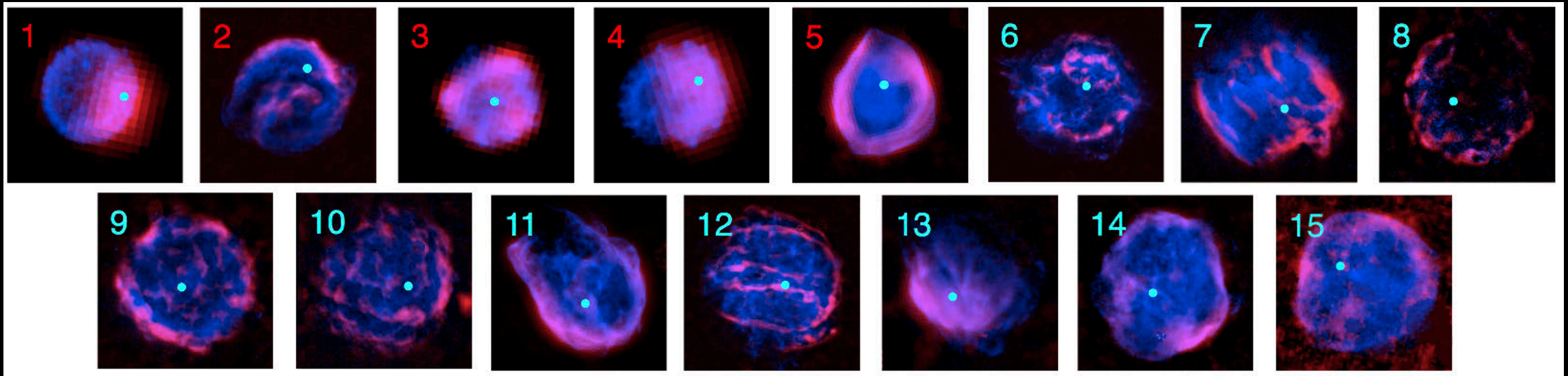
20 cm



References: TeV: HESS Collaboration 2016; X-ray: Lopez et al. 2013; [Fe II] and H₂: Keohane et al. 2007; 24 μm : Koo et al. 2016; 20 cm: Helfand et al. 2006

Other Wavebands: Infrared

X-rays
IR



Peters, Lopez et al. 2013

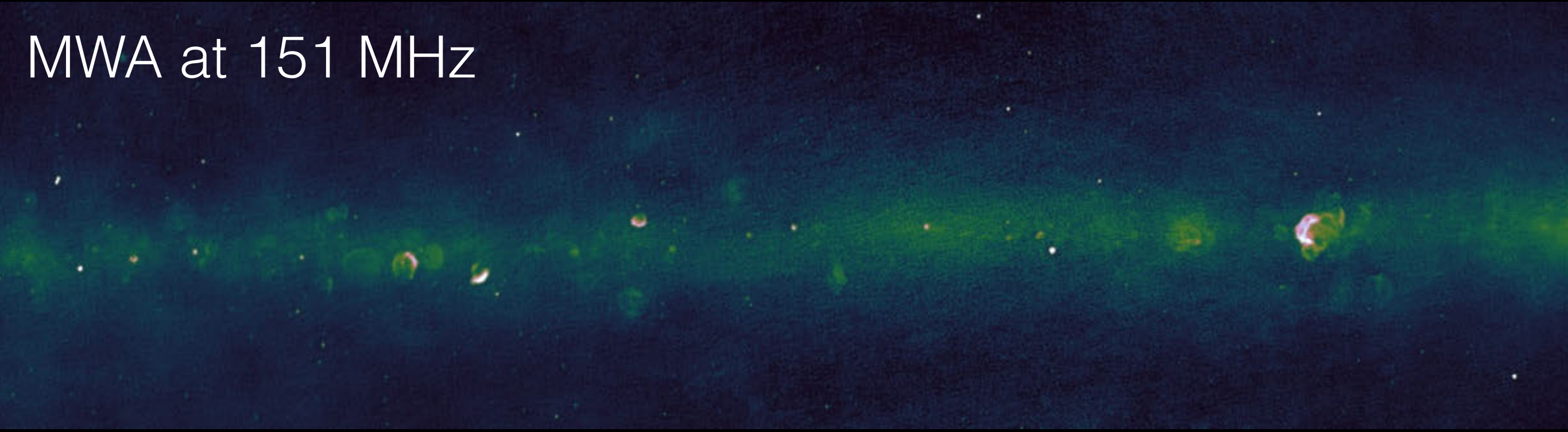


Charee Peters,
U Wisconsin
PhD Student

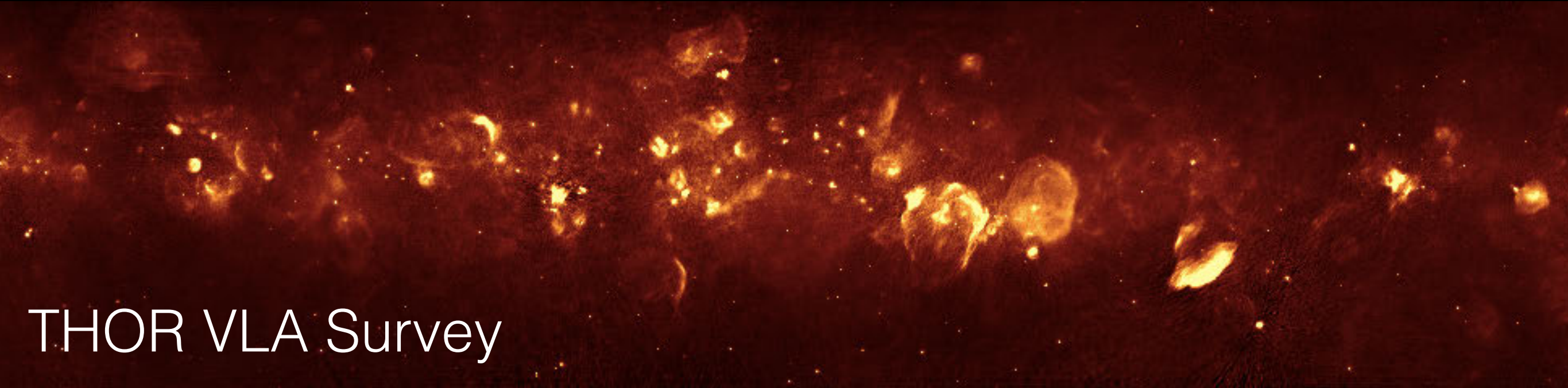
Other Wavebands: Radio

Galactic SNRs are mostly found in the radio

MWA at 151 MHz

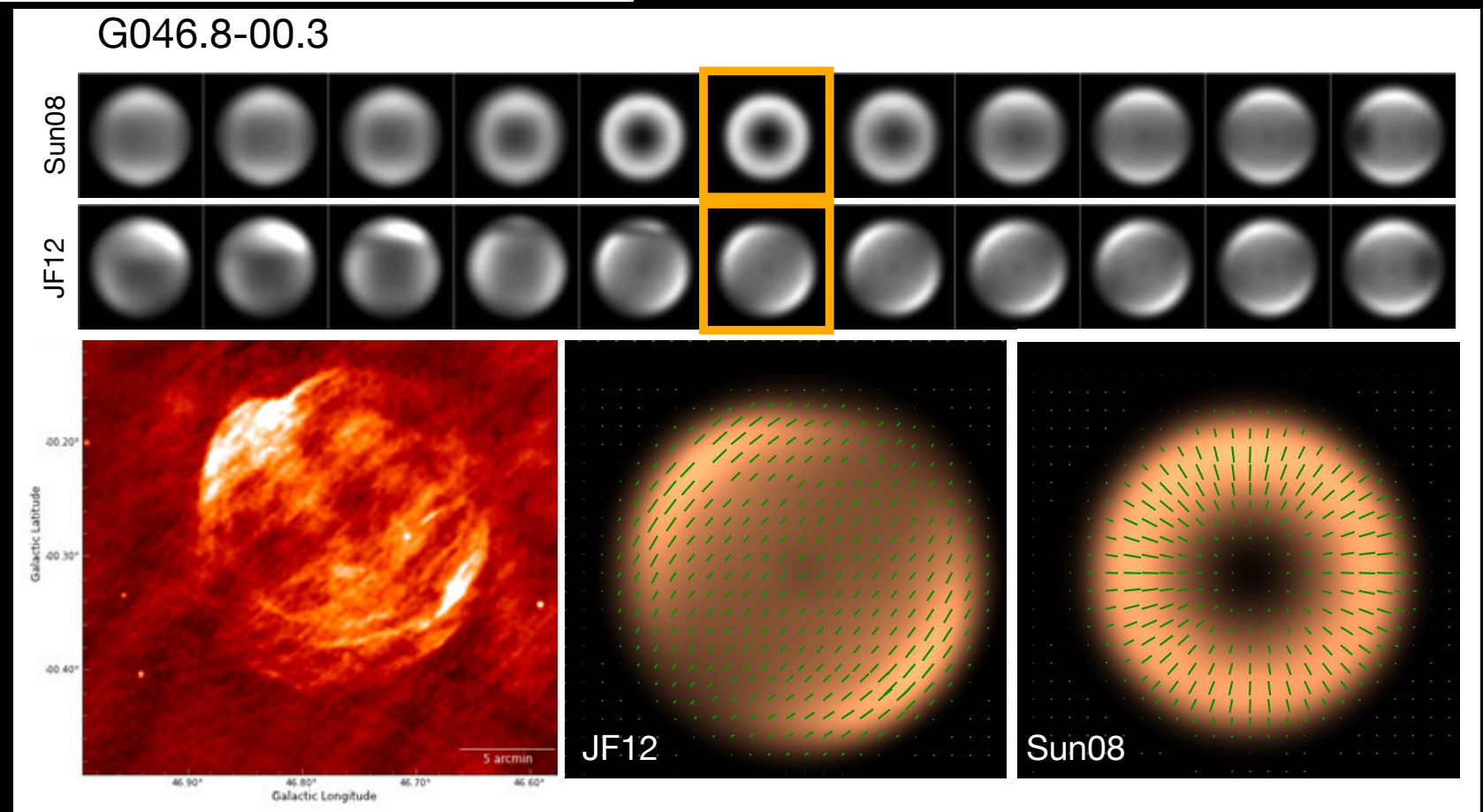
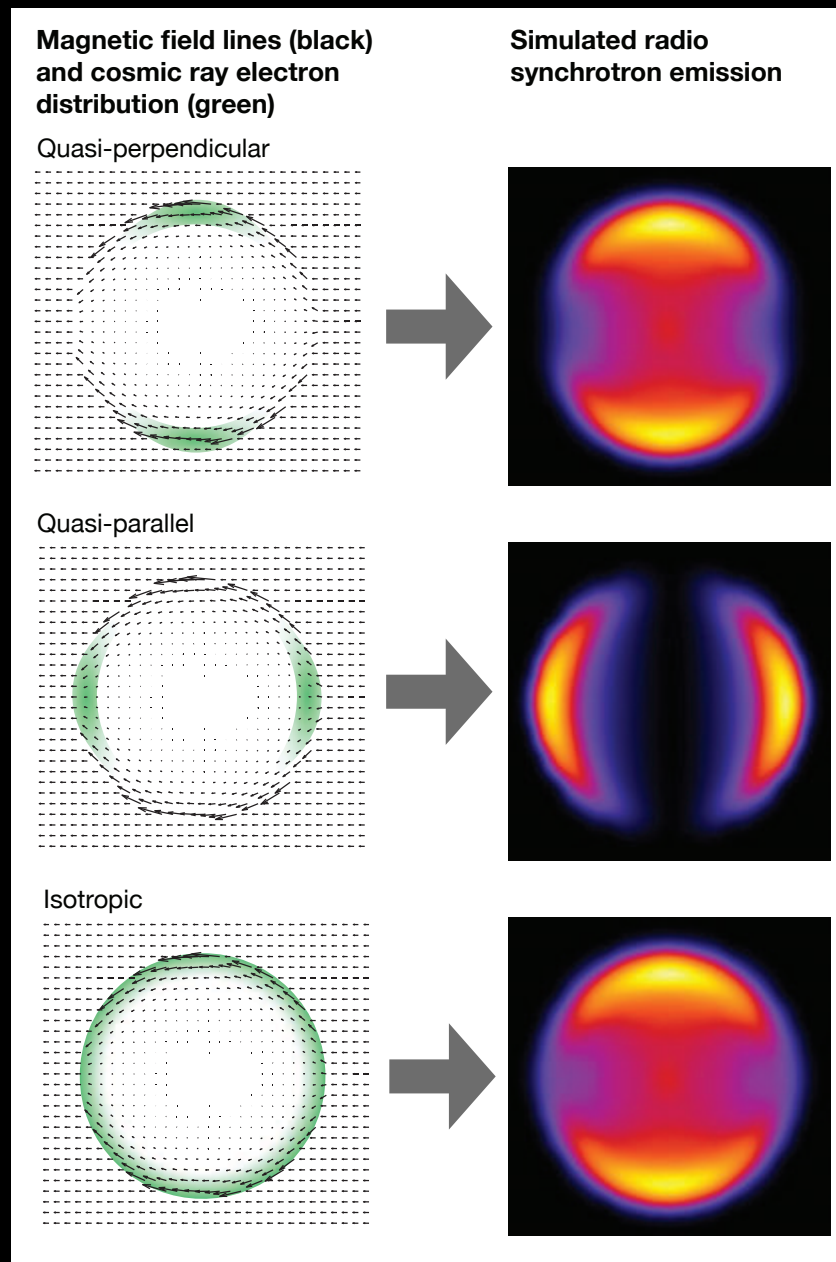
A radio image showing a horizontal band of greenish emission against a dark blue background. The emission is concentrated in a narrow band across the center of the frame, with several distinct, bright spots and structures visible within the band.

THOR VLA Survey

A radio image showing a dense field of orange and yellow emission structures. The structures are concentrated in a horizontal band across the center of the frame, with many bright spots and complex, irregular shapes. The background is dark brown.

Other Wavebands: Radio

Morphology of synchrotron emission in radio yields information about the ambient density, B-field, and cosmic-ray acceleration



West et al. 2016

See also Orlando et al. 2007, Schneider et al. 2015, West et al. 2017

Other Wavebands: Radio

Simulations show that degree of asymmetry changes with time in a turbulent/inhomogeneous medium (e.g., Kim & Ostriker 2015, Martizzi et al. 2015, Walch & Naab 2015, Zhang & Chevalier 2019)

Other Wavebands: Radio

Simulations show that degree of asymmetry changes with time in a turbulent/inhomogeneous medium (e.g., Kim & Ostriker 2015, Martizzi et al. 2015, Walch & Naab 2015, Zhang & Chevalier 2019)

Does radio morphology change with age?

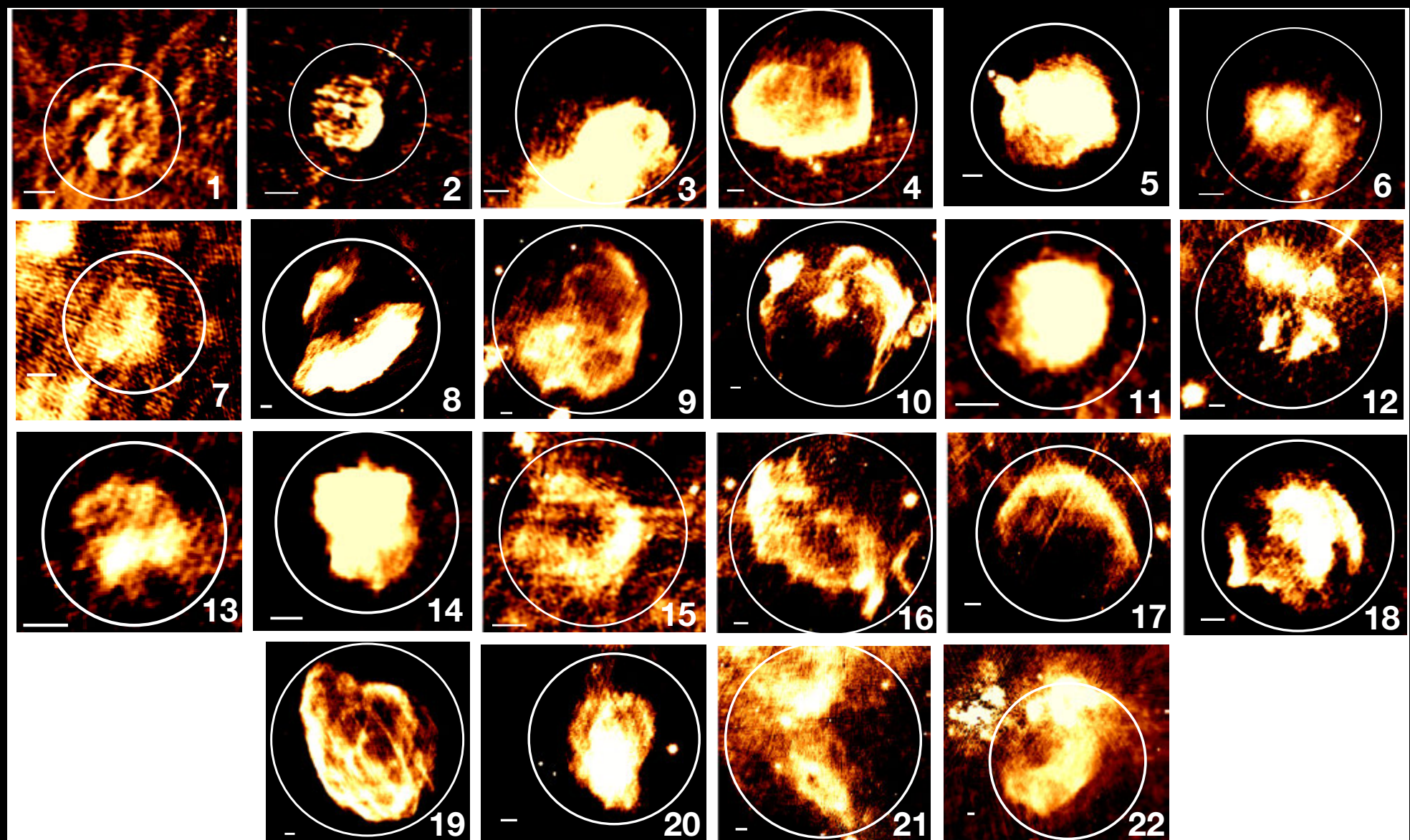
Other Wavebands: Radio

Simulations show that degree of asymmetry changes with time in a turbulent/inhomogeneous medium (e.g., Kim & Ostriker 2015, Martizzi et al. 2015, Walch & Naab 2015, Zhang & Chevalier 2019)

Does radio morphology change with age?



Jennifer
Stafford,
OSU
Undergrad



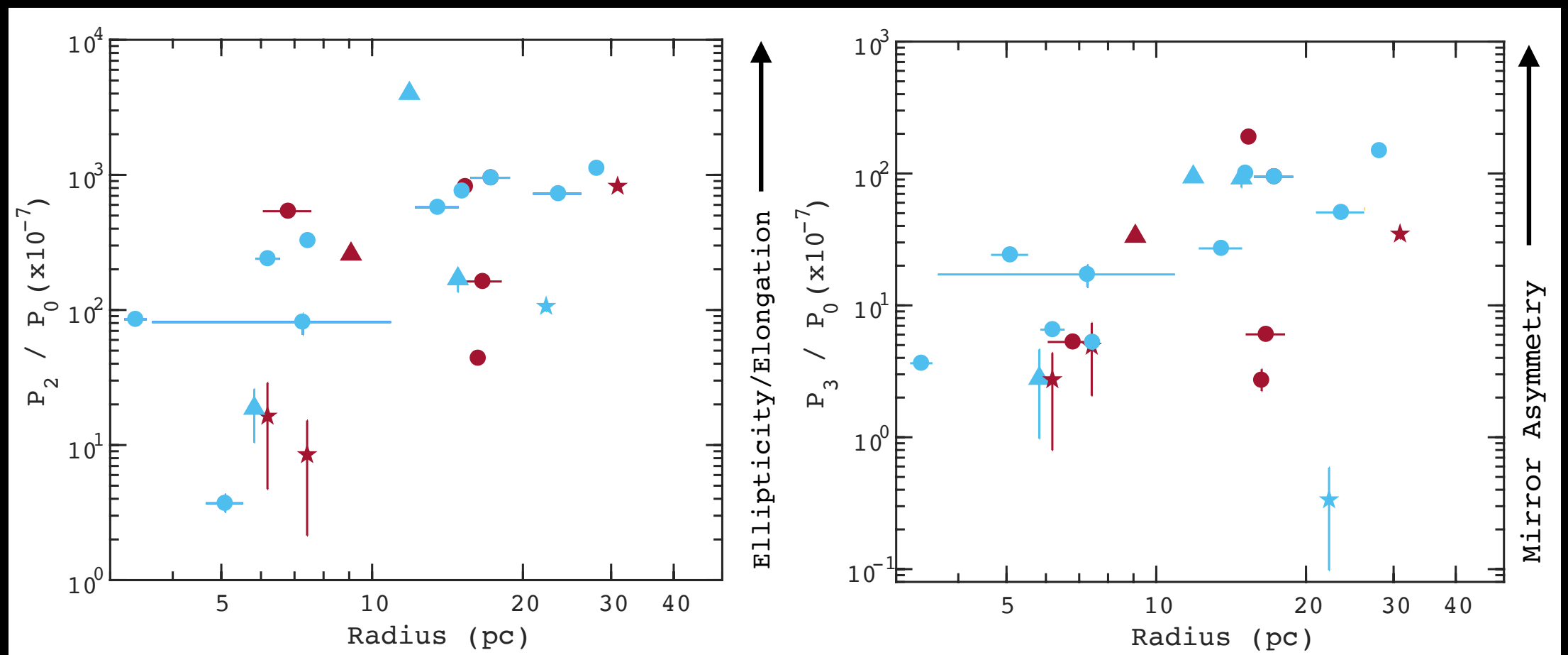


Jennifer
Stafford,
OSU
Undergrad

Other Wavebands: Radio

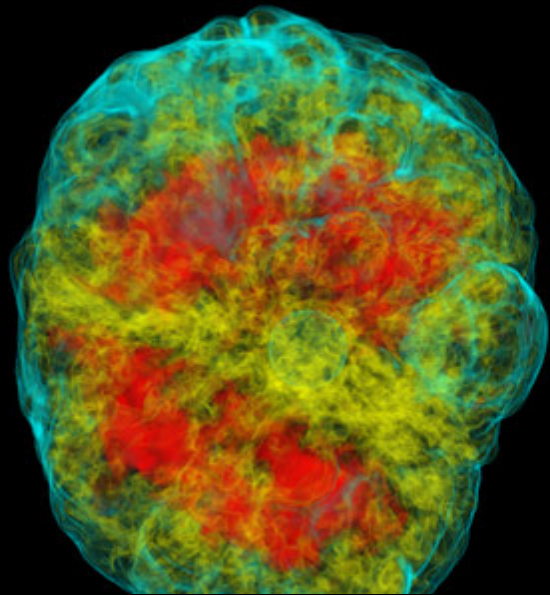
In radio, SNRs get more asymmetric with size/age, consistent with expansion into an inhomogeneous/turbulent ISM

Currently extending this approach to a larger sample (~ 100 SNRs) in radio

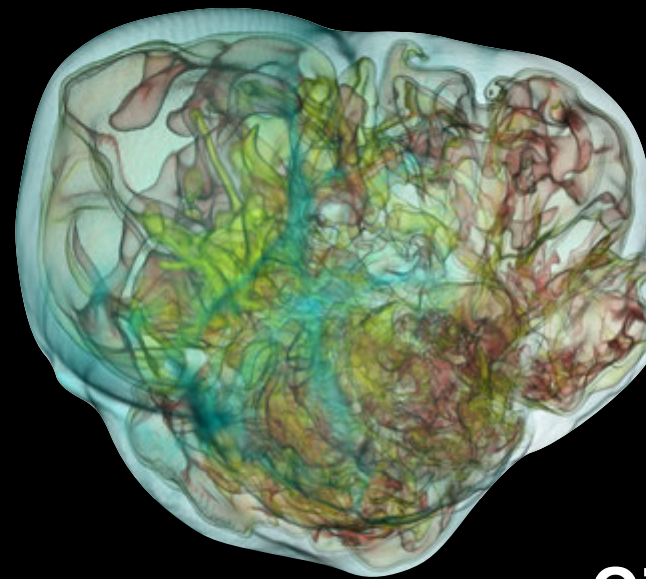


Tying Morphologies to Originating Explosions

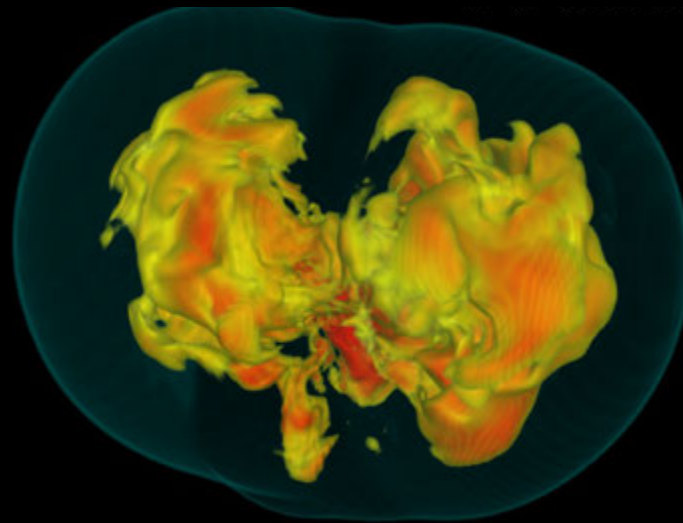
Roberts et al. (2016)



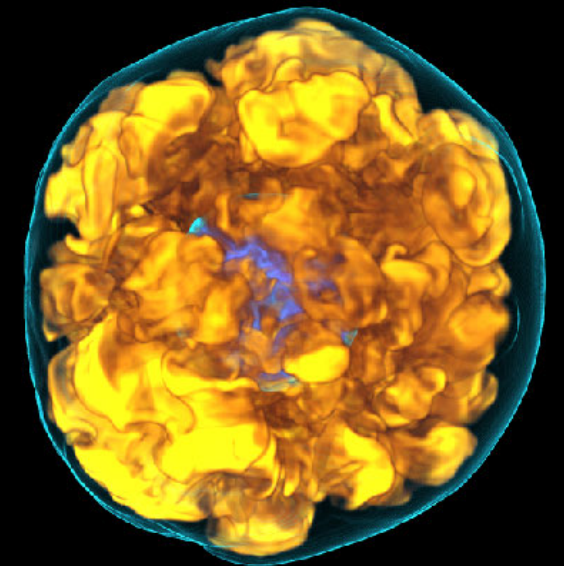
Lentz et al. (2016)



Janka et al. (2016)



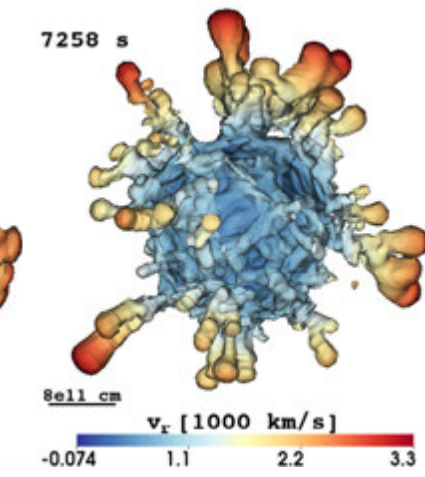
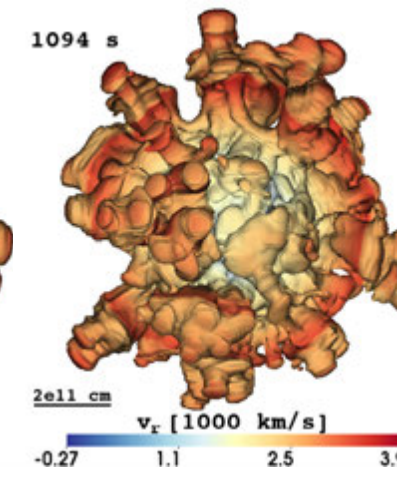
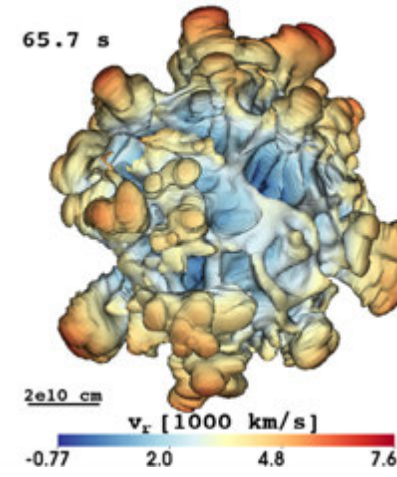
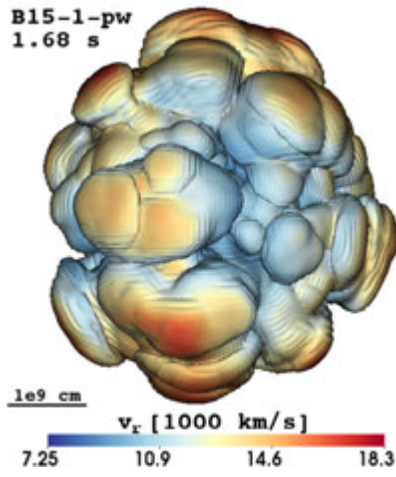
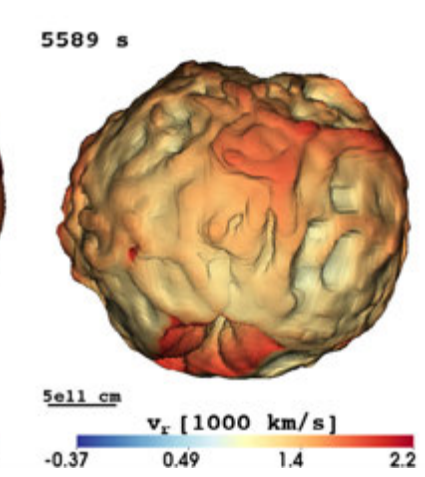
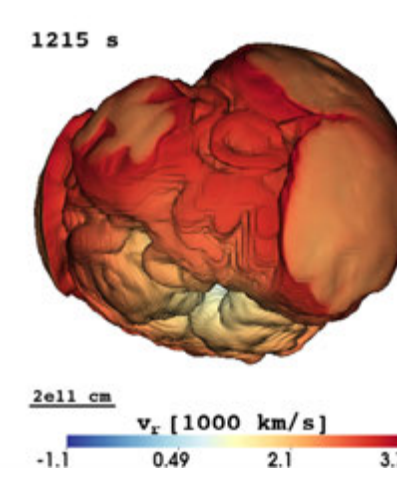
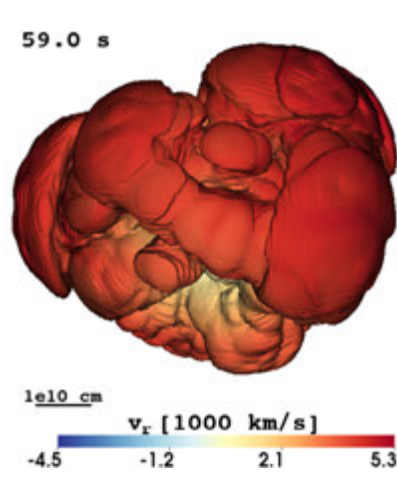
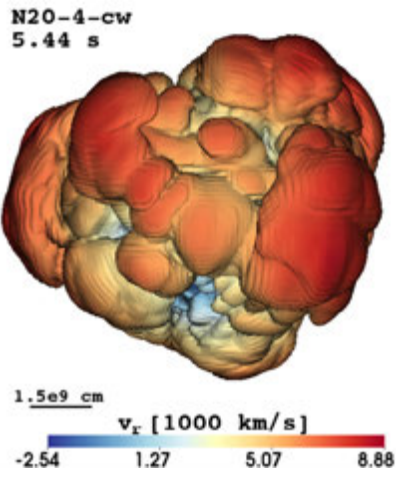
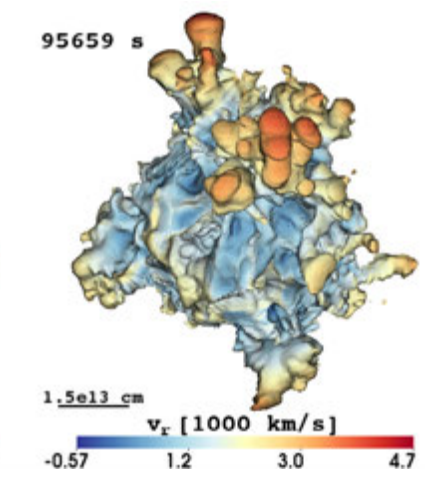
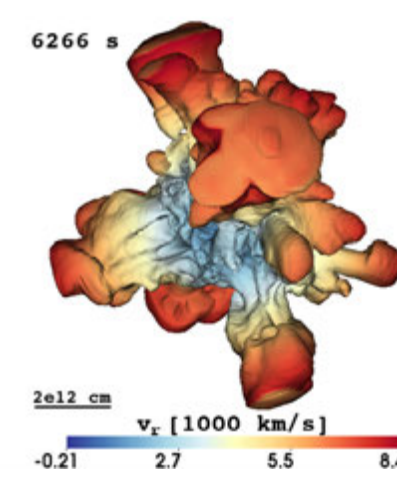
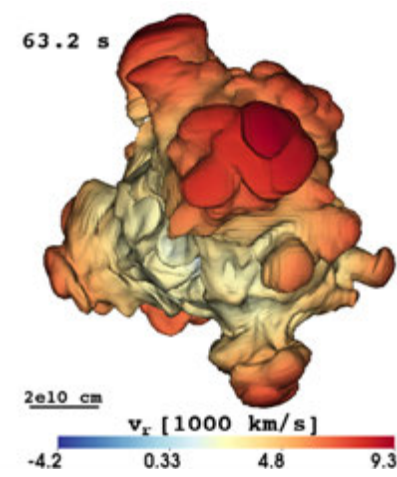
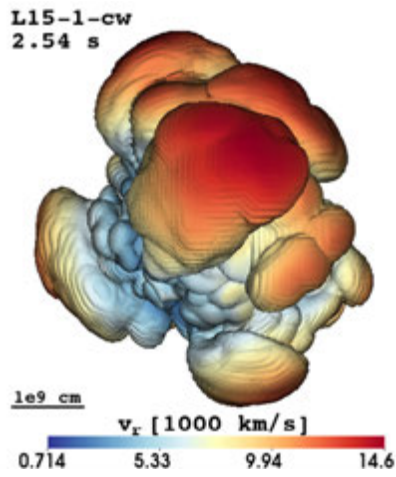
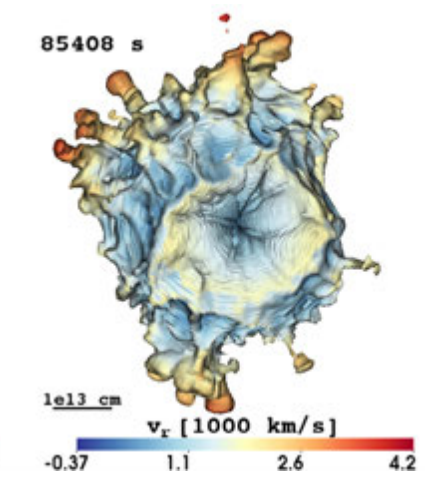
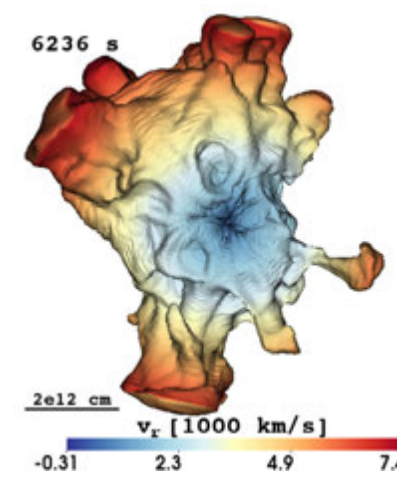
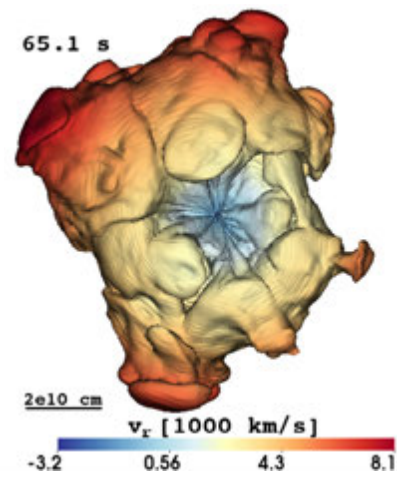
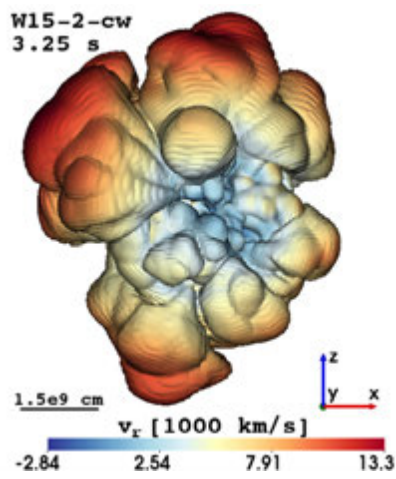
O'Connor & Couch 2018



Simulations are yielding predictions about ejecta distributions, large-scale compositional asymmetries, neutron star kicks that can be compared to observations.

Ni-56 Distribution Depends on Progenitor Structure

Wongwathanarat et al. 2015



Comparing Elemental Spatial Distributions

Do different elements get ejected differently?



Tyler Holland-
Ashford,
OSU
Graduate
Student

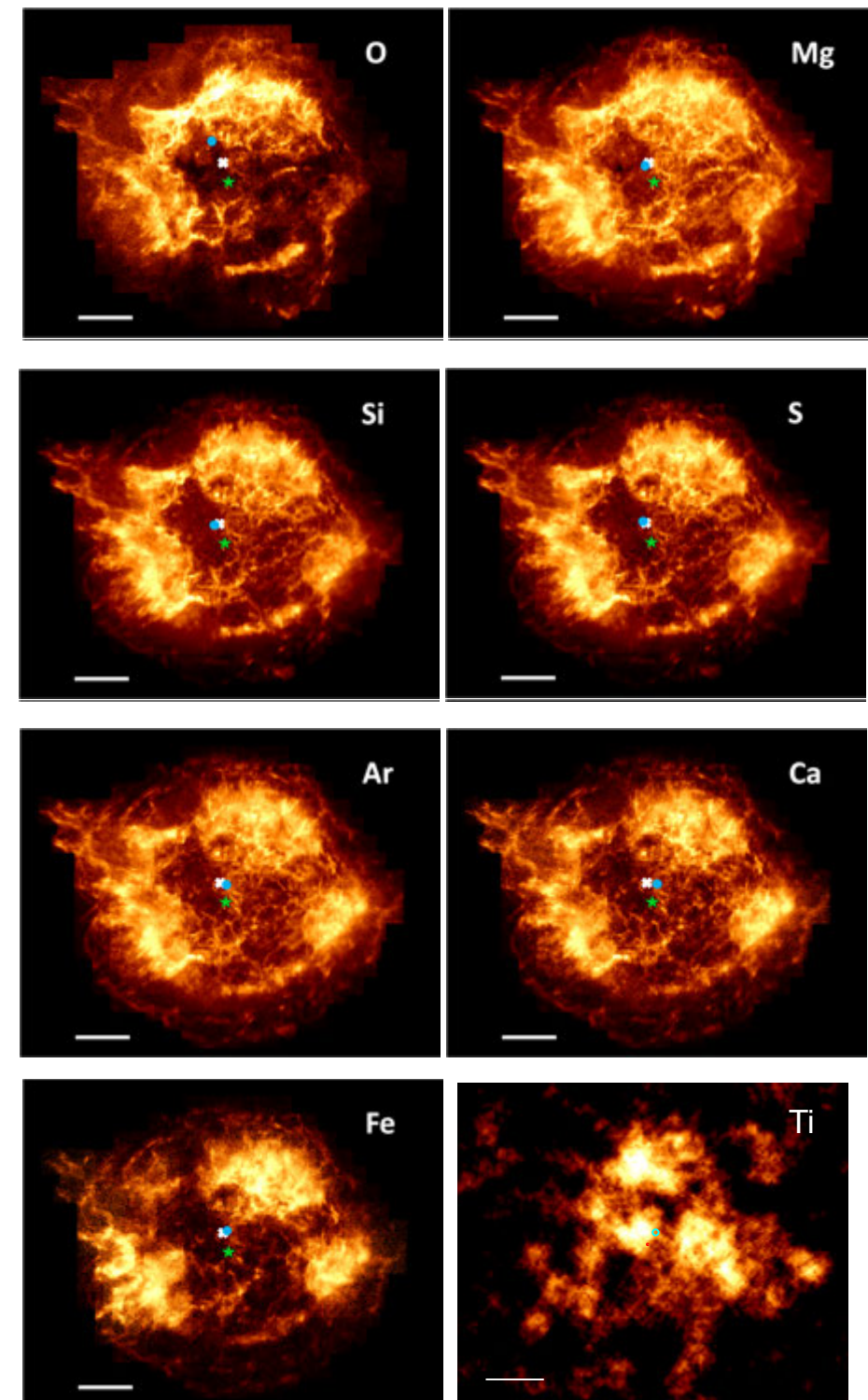
Comparing Elemental Spatial Distributions

Do different elements get ejected differently?



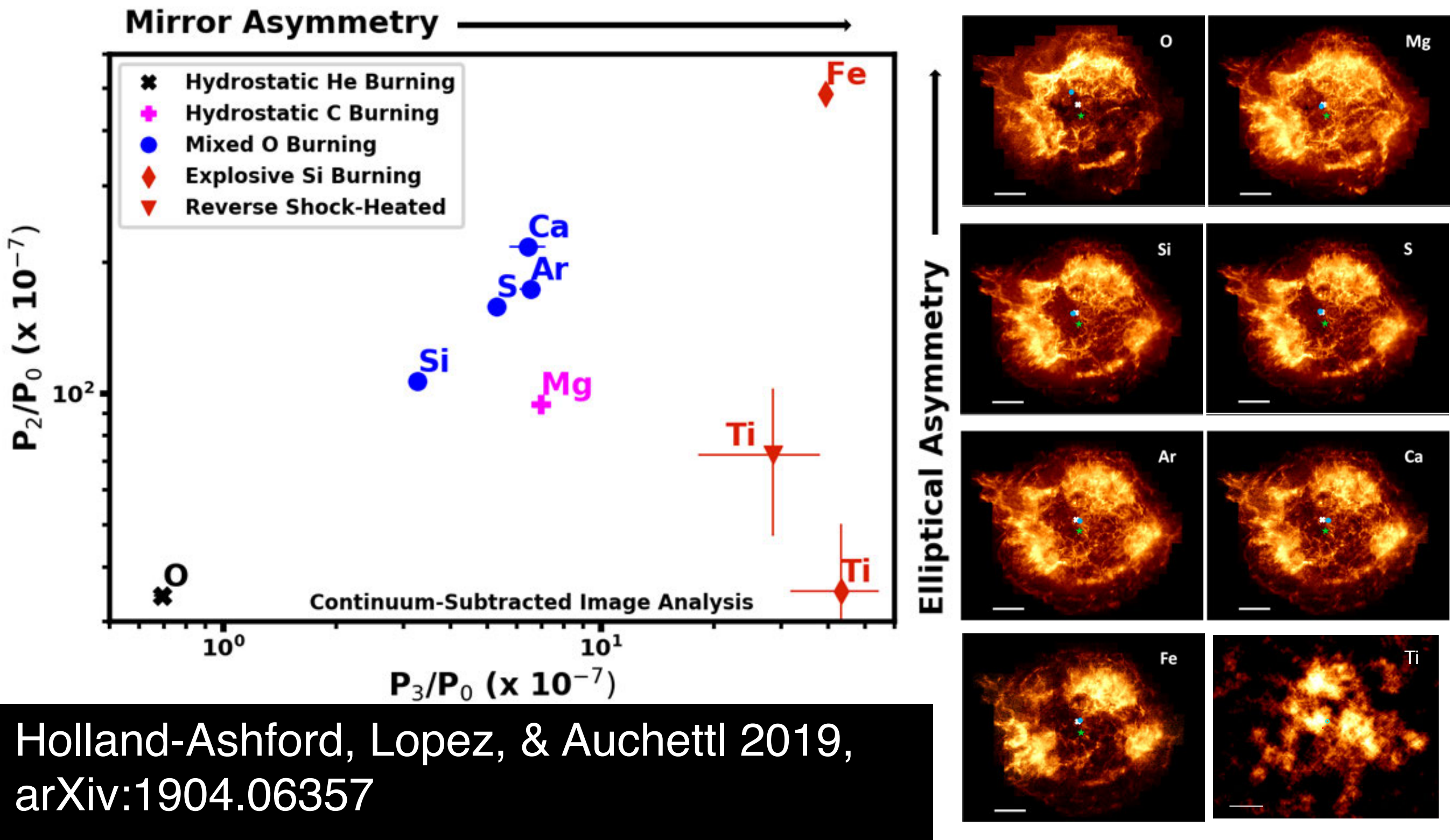
Tyler Holland-Ashford,
OSU
Graduate
Student

Holland-Ashford, Lopez, & Auchetti 2019,
arXiv:1904.06357



Comparing Elemental Spatial Distributions

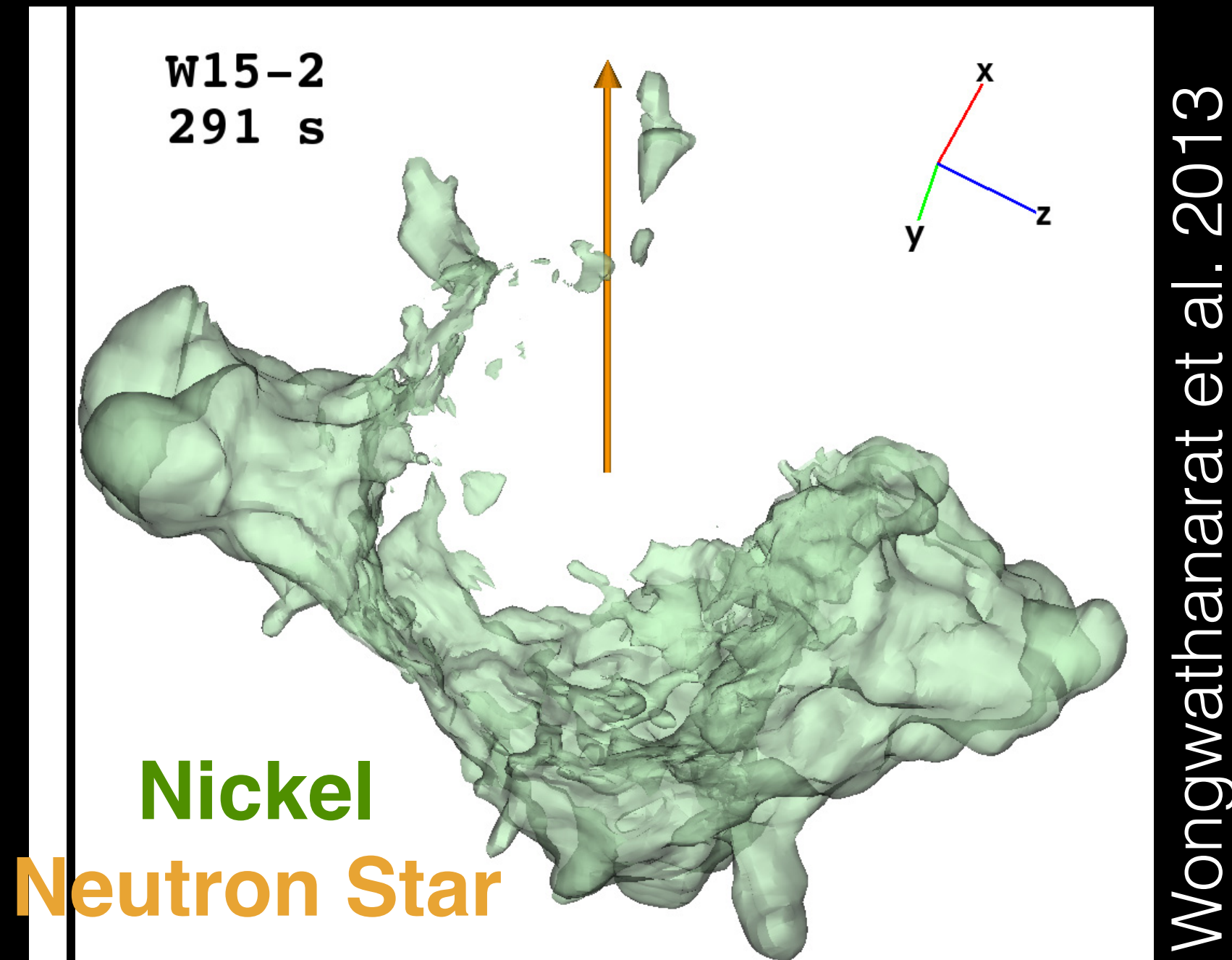
Do different elements get ejected differently?



Holland-Ashford, Lopez, & Auchetti 2019,
arXiv:1904.06357

Burning processes from Woosley, Heger, Weaver 2002; Curtis et al. 2019

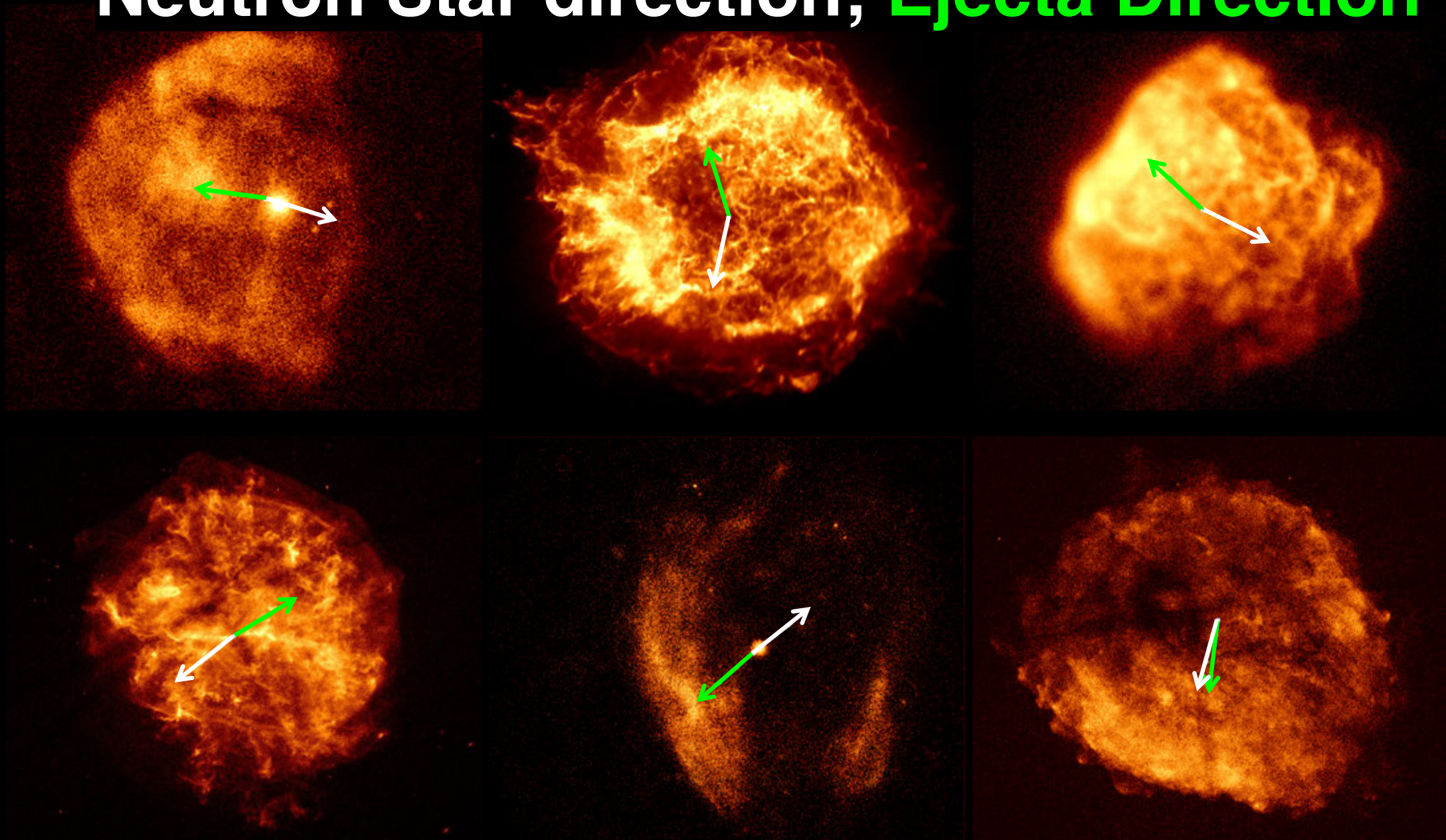
Neutron Star Kicks



If NS kick arises from asymmetric mass ejection (Scheck et al. 2006, Wongwathanarat et al. 2013, Janka 2017), NS goes opposite to heavy ejecta. If NS arises from anisotropic neutrino emission (Fryer & Kusenko 2006), NS goes in the same direction as heavy ejecta.

Neutron Stars Kicked Opposite to Ejecta

Neutron Star direction; **Ejecta Direction**



Holland-Ashford, Lopez et al. 2017

Neutron stars are 'kicked' by the SN explosion opposite to the ejected material. See also Katsuda et al. 2018

Type Ia Progenitor Systems: the Debate

Ways to distinguish single vs. double degenerate scenarios:

1. Existing populations of potential progenitors
2. Pre-explosion data of SN Ia sites find no companions
3. Observed properties of SNe Ia events themselves
4. Signs of circumstellar medium interaction
5. SNe Ia time delay distribution

Maoz, Mannucci & Nelemans 2014

Type Ia Progenitor Systems: the Debate

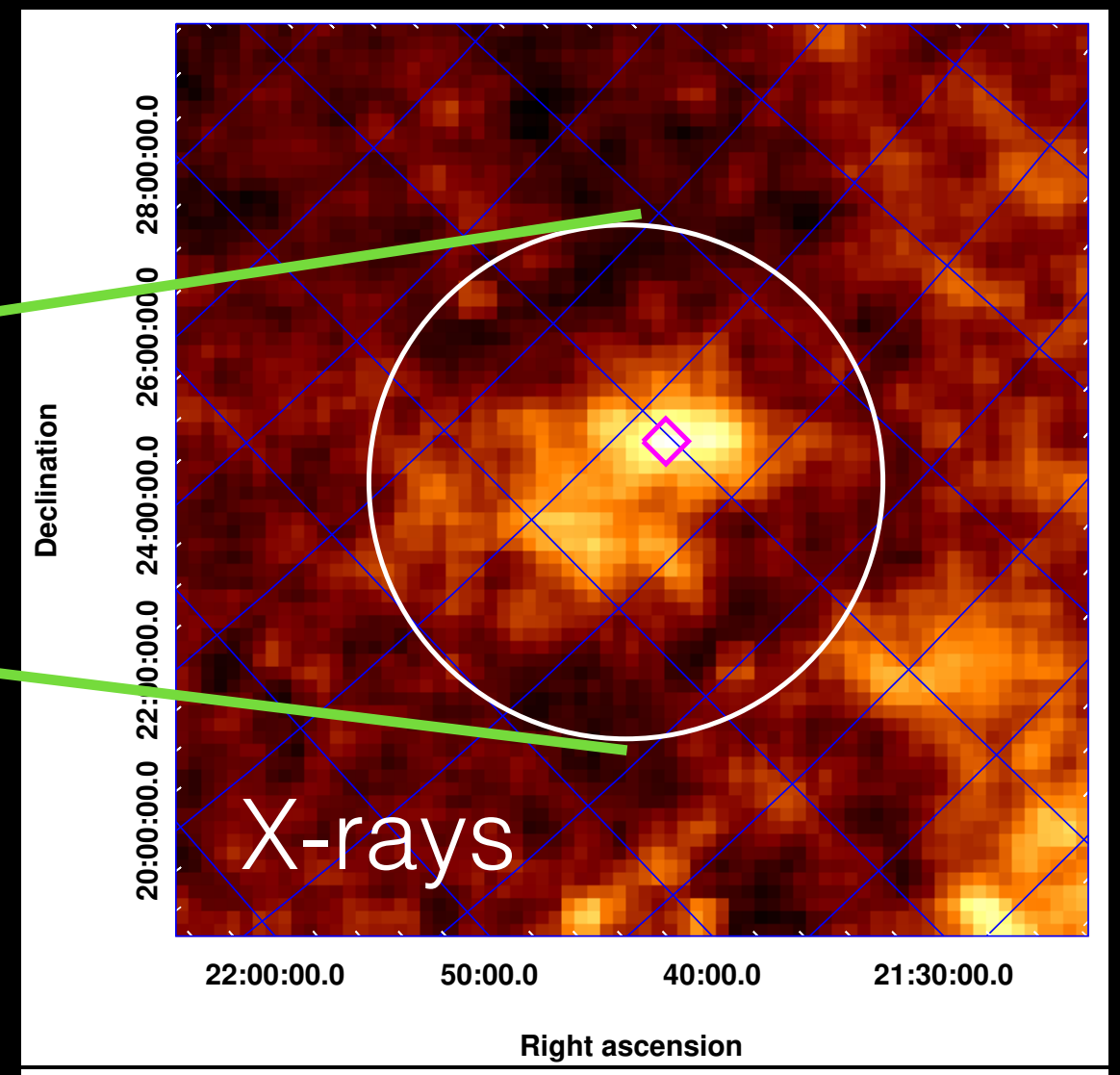
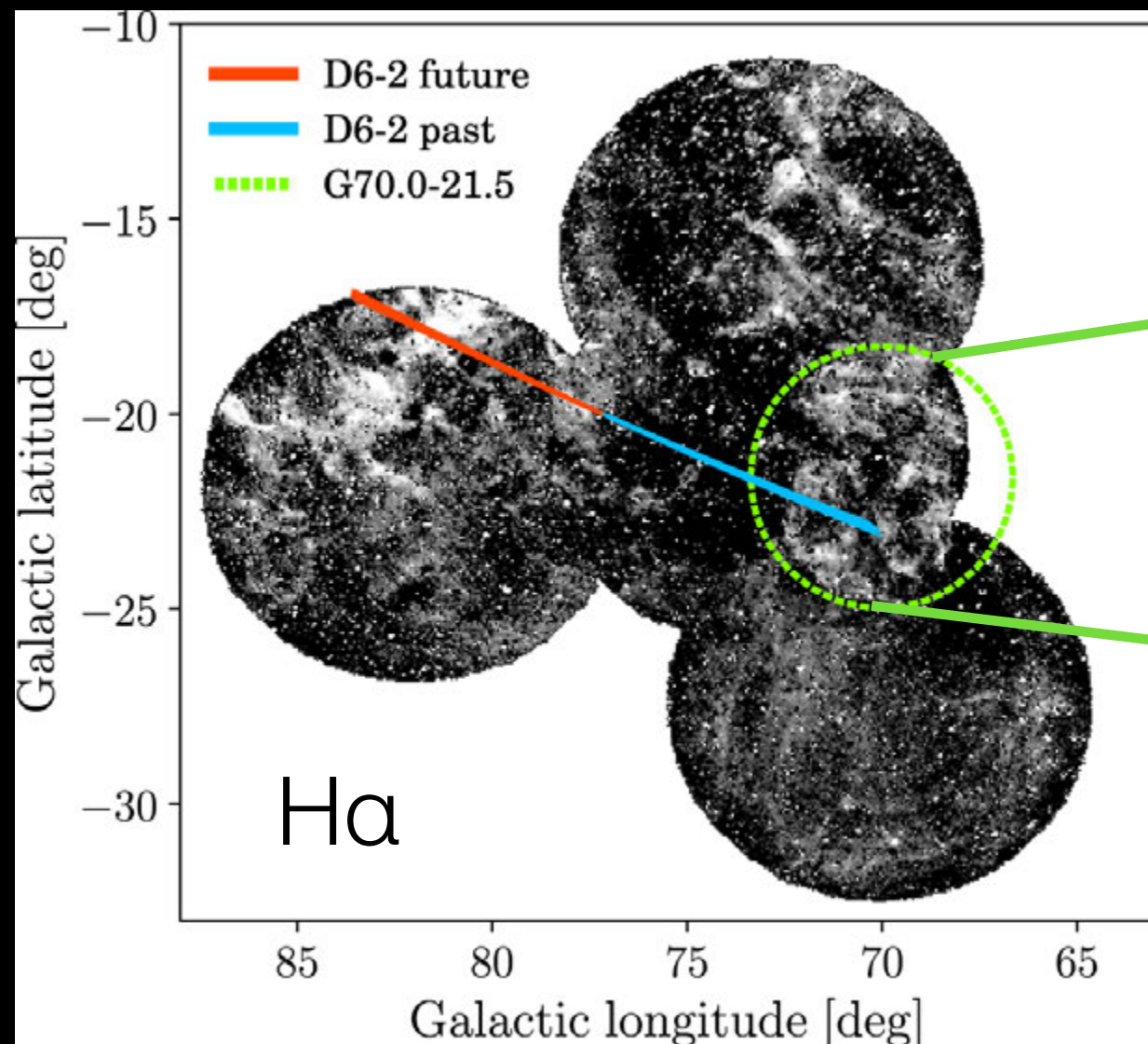
SNRs can offer insights in a variety of ways:

1. Search for surviving companions (e.g., Schaefer & Pagnotta 2012, Kerzendorf et al. 2019) - haven't found any
2. Nucleosynthesis - compare heavy element abundances to yields in different progenitor systems/ignition processes (e.g., Lopez et al. 2015; Yamaguchi et al. 2015)
3. Signs of circumstellar interactions (see reviews by Patnaude & Badenes 2017 and Vink 2017)
4. Hypervelocity white dwarfs originating from SNRs

Type Ia Progenitor Systems: High-Velocity White Dwarfs

Shen+18 searched for hypervelocity WDs in Gaia DR2 and found three.

One traces back to the position of a known SNR, G70.0-21.5 and originated from there $\sim 90,000$ years ago.



Type Ia Progenitor Systems: the Debate

SNRs can offer insights in a variety of ways:

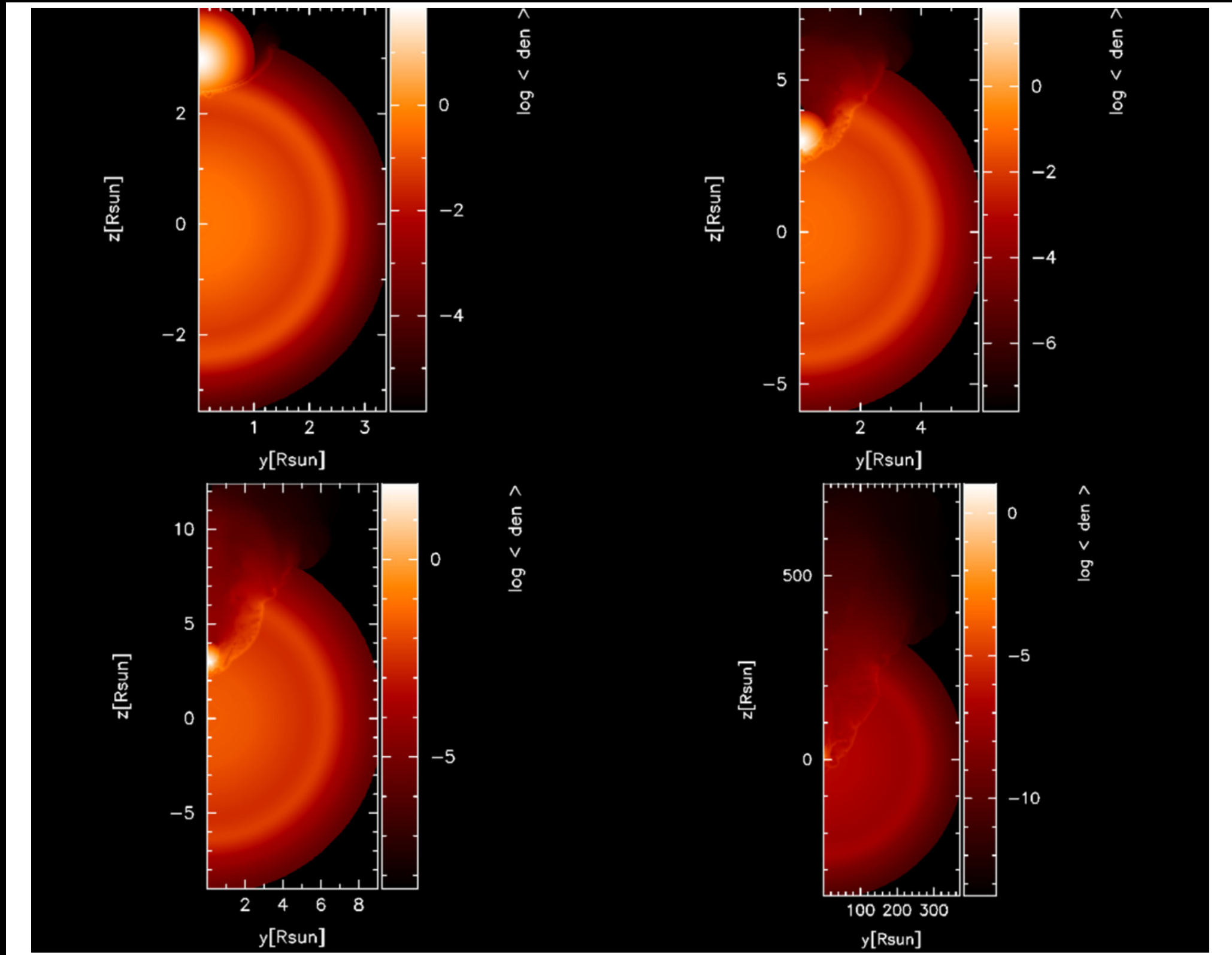
1. Search for surviving companions (e.g., Schaefer & Pagnotta 2012, Kerzendorf et al. 2019) - haven't found any
2. Nucleosynthesis - compare heavy element abundances to yields in different progenitor systems/ignition processes (e.g., Lopez et al. 2015; Yamaguchi et al. 2015)
3. Signs of circumstellar interactions (see reviews by Patnaude & Badenes 2017 and Vink 2017)
4. Hypervelocity white dwarfs originating from SNRs

Type Ia Progenitor Systems: the Debate

SNRs can offer insights in a variety of ways:

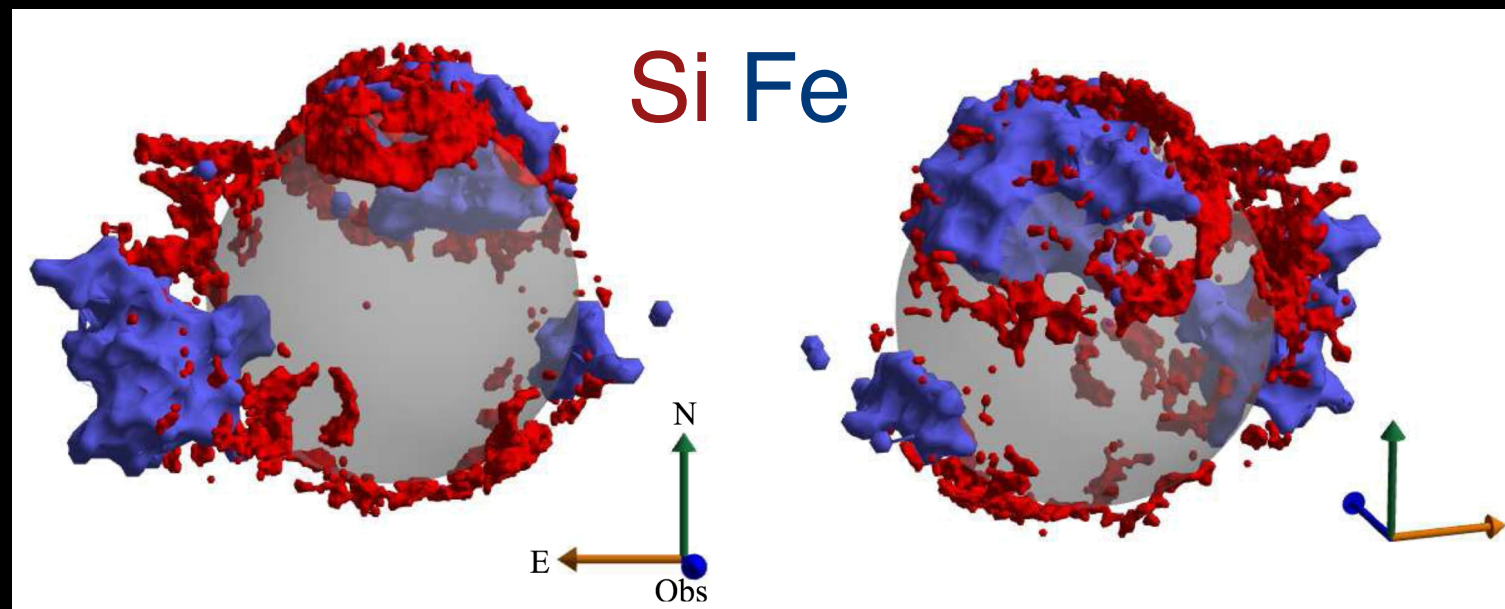
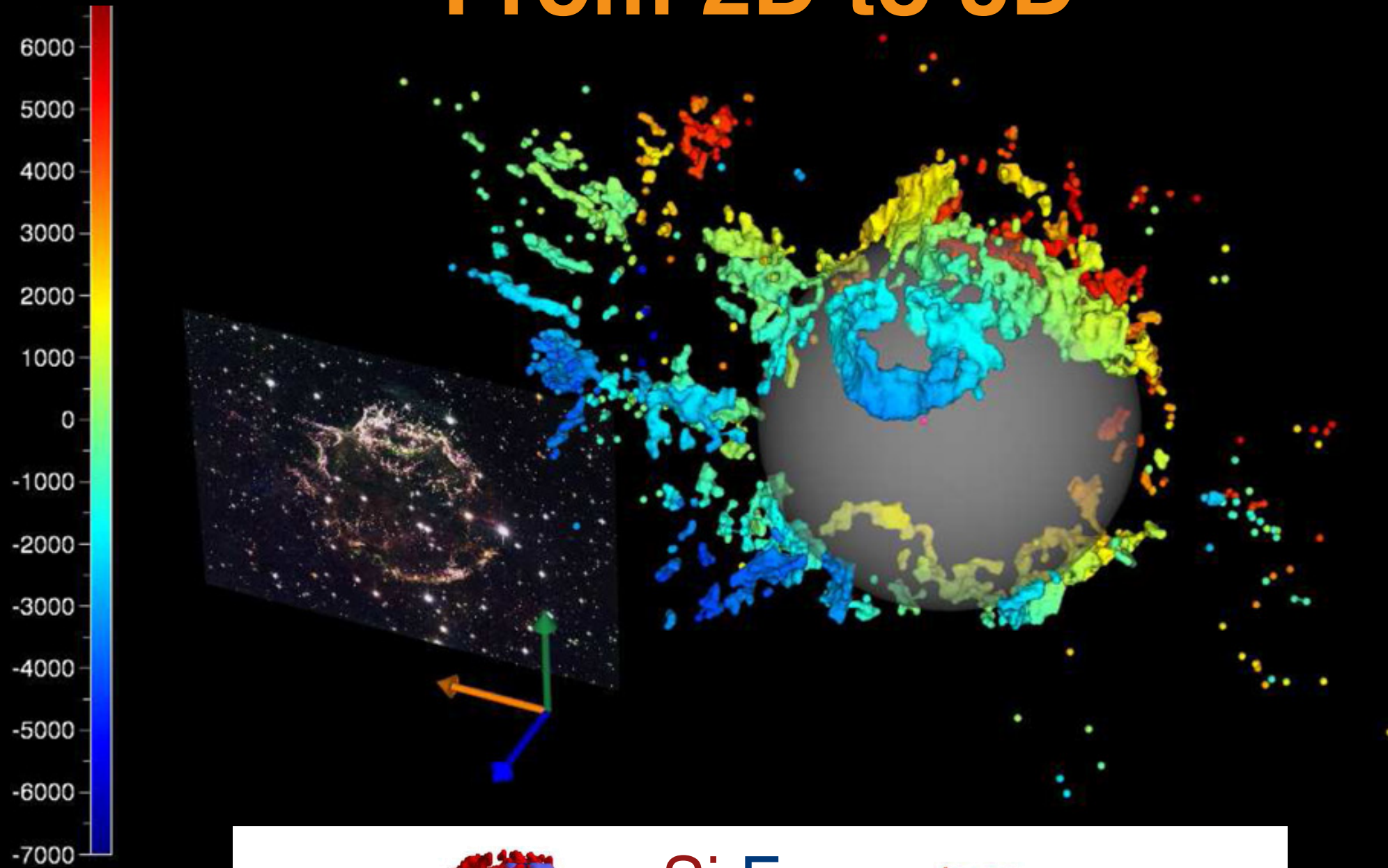
1. Search for surviving companions (e.g., Schaefer & Pagnotta 2012, Kerzendorf et al. 2019) - haven't found any
2. Nucleosynthesis - compare heavy element abundances to yields in different progenitor systems/ignition processes (e.g., Lopez et al. 2015; Yamaguchi et al. 2015)
3. Signs of circumstellar interactions (see reviews by Patnaude & Badenes 2017 and Vink 2017)
4. Hypervelocity white dwarfs originating from SNRs
5. Morphologies - single vs. double will produce different shapes

Holes/Gaps in Type Ia SNRs - Possible Signature of Single-Degenerate Scenario

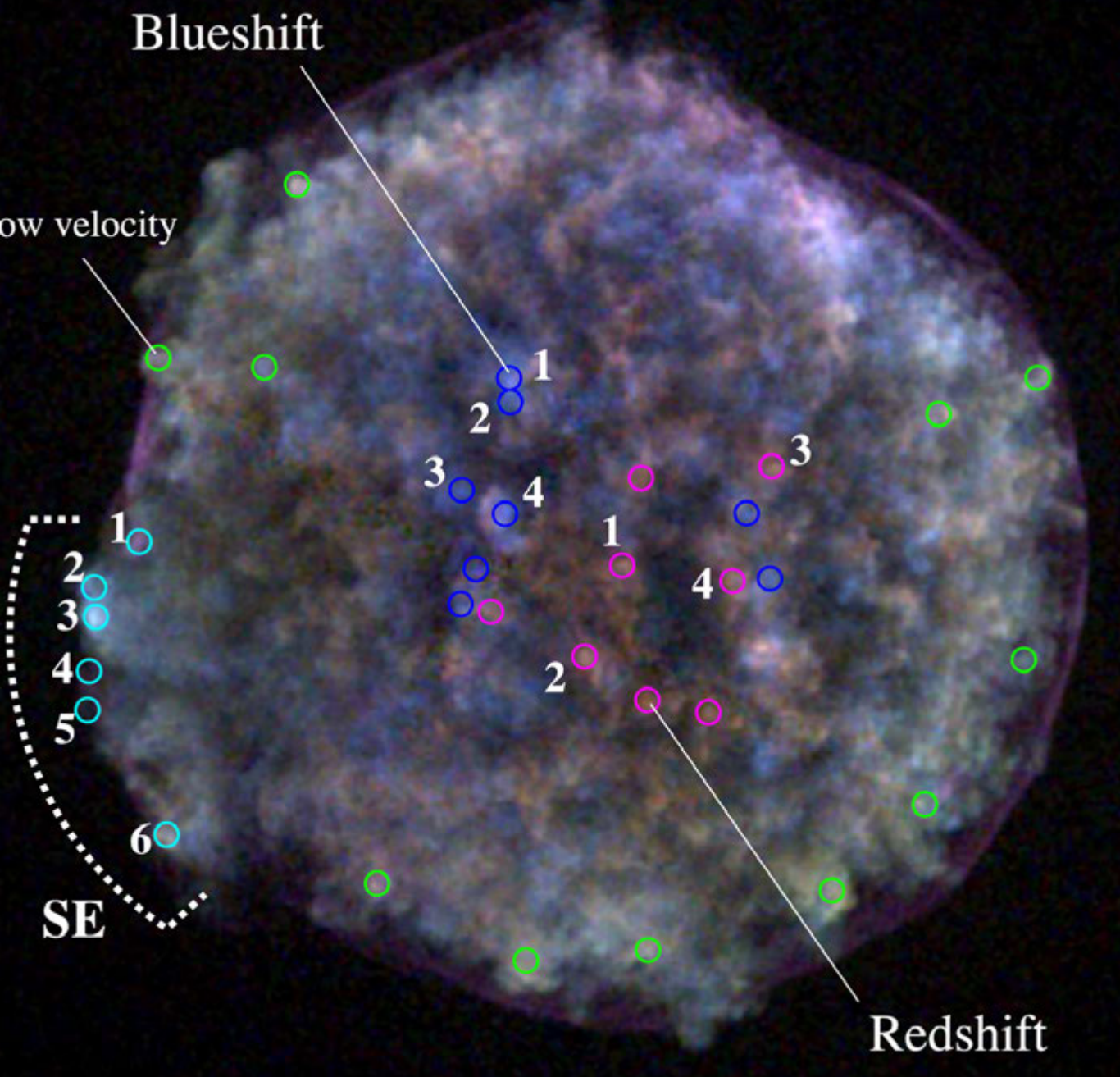


Garcia-Senz et al. 2012

From 2D to 3D



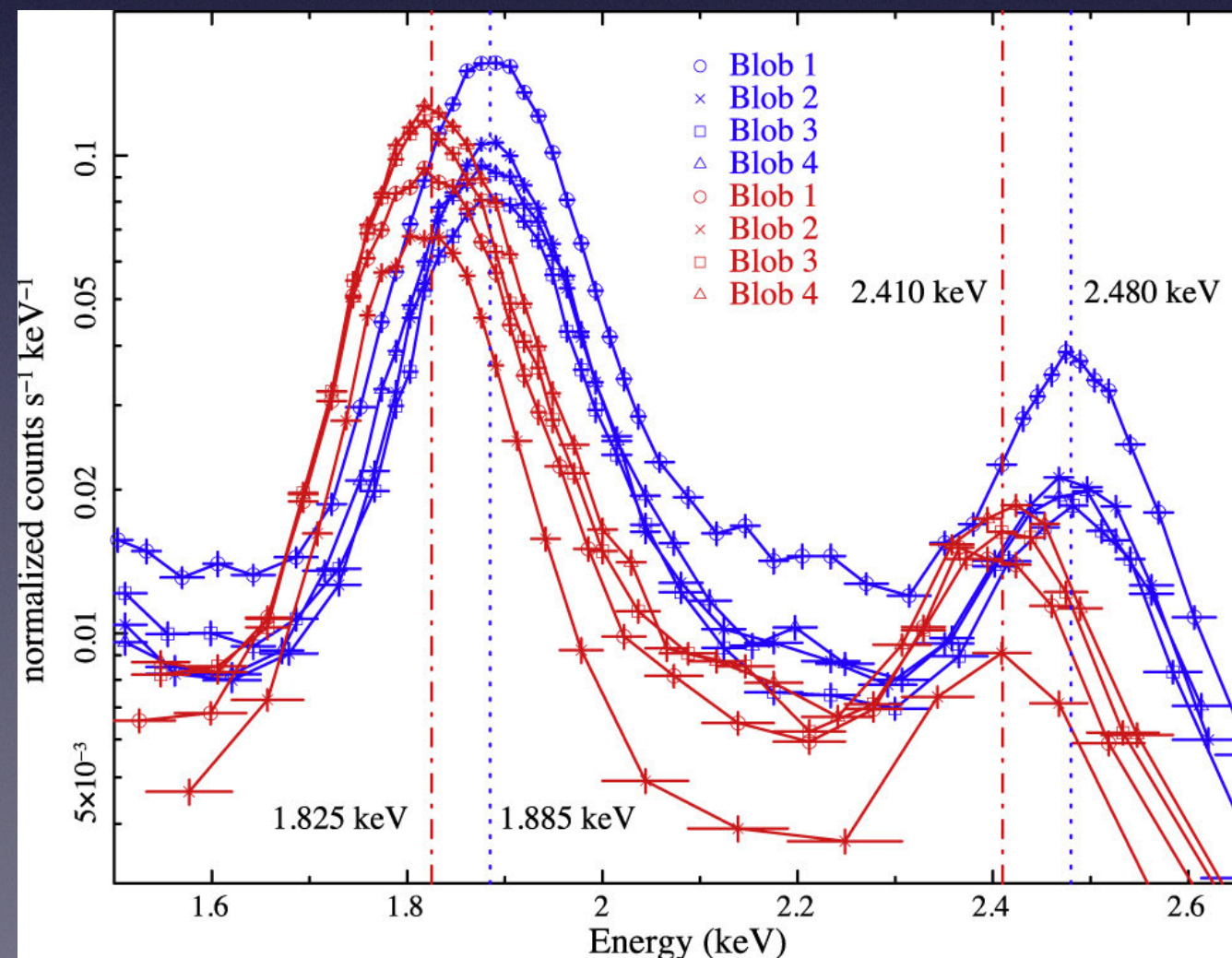
Milisavljevic & Fesen 2013



Tycho's SNR

Spectral analysis of small knots of ejecta in Tycho show very high line-of-sight velocities

Blueshifted mean = -3220 km/s
Redshifted mean = 4980 km/s

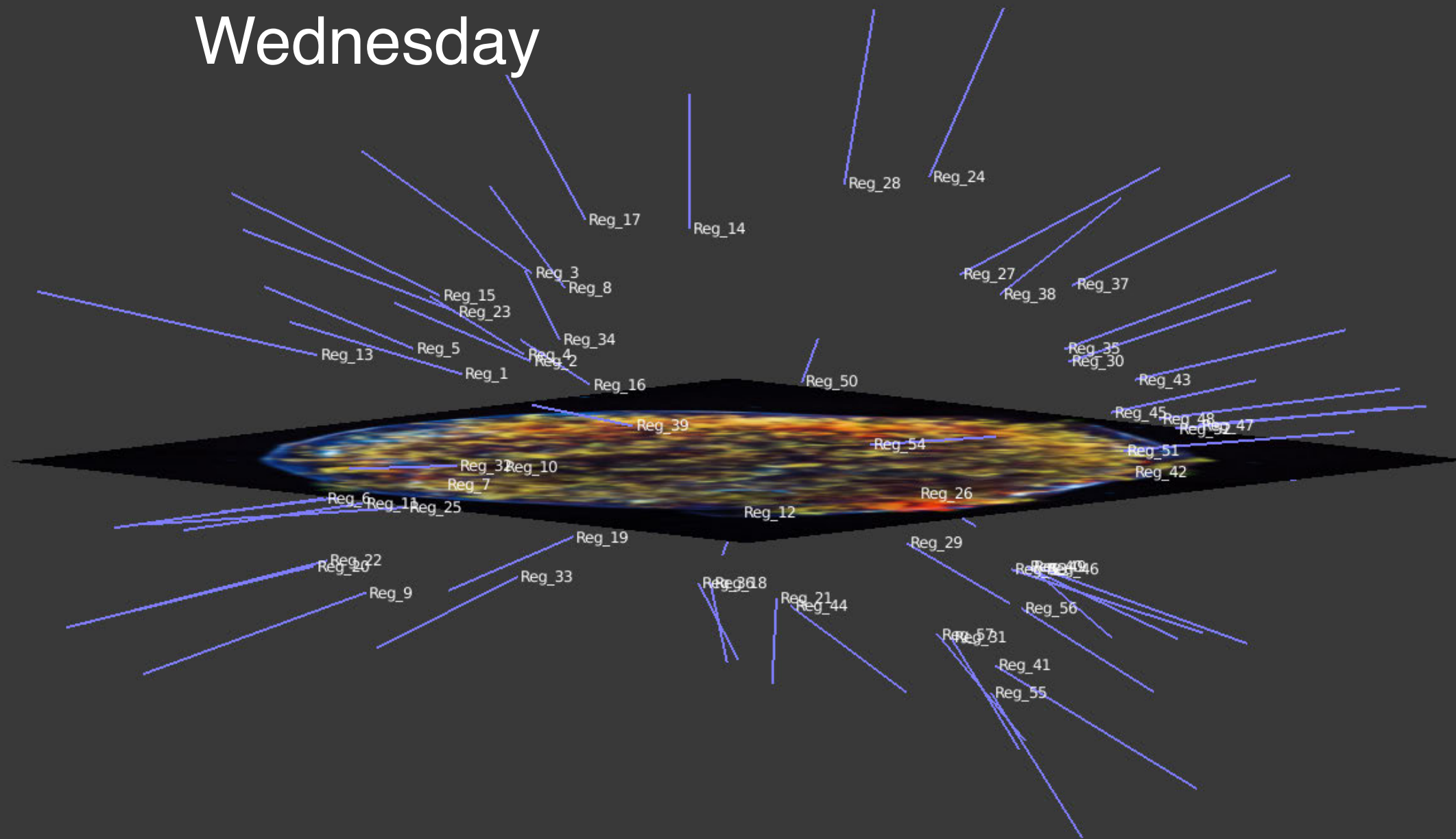


See Sato & Hughes 2017

From Brian Williams talk on
Wednesday

Results and 3D visualization

From Brian Williams talk on
Wednesday



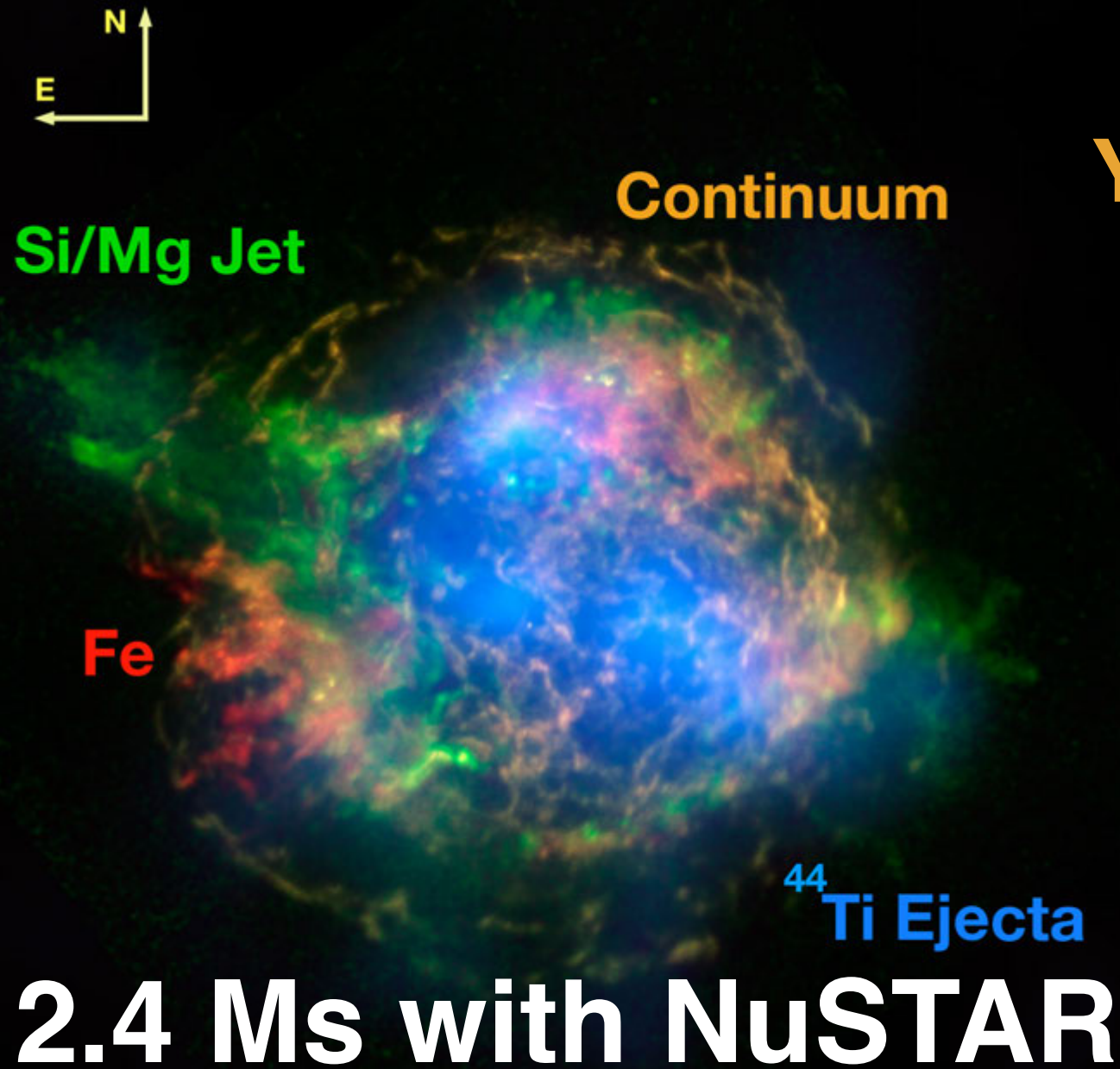
Velocity vectors are of arbitrary absolute length, but
are scaled accurately relative to each other!

From 2D to 3D

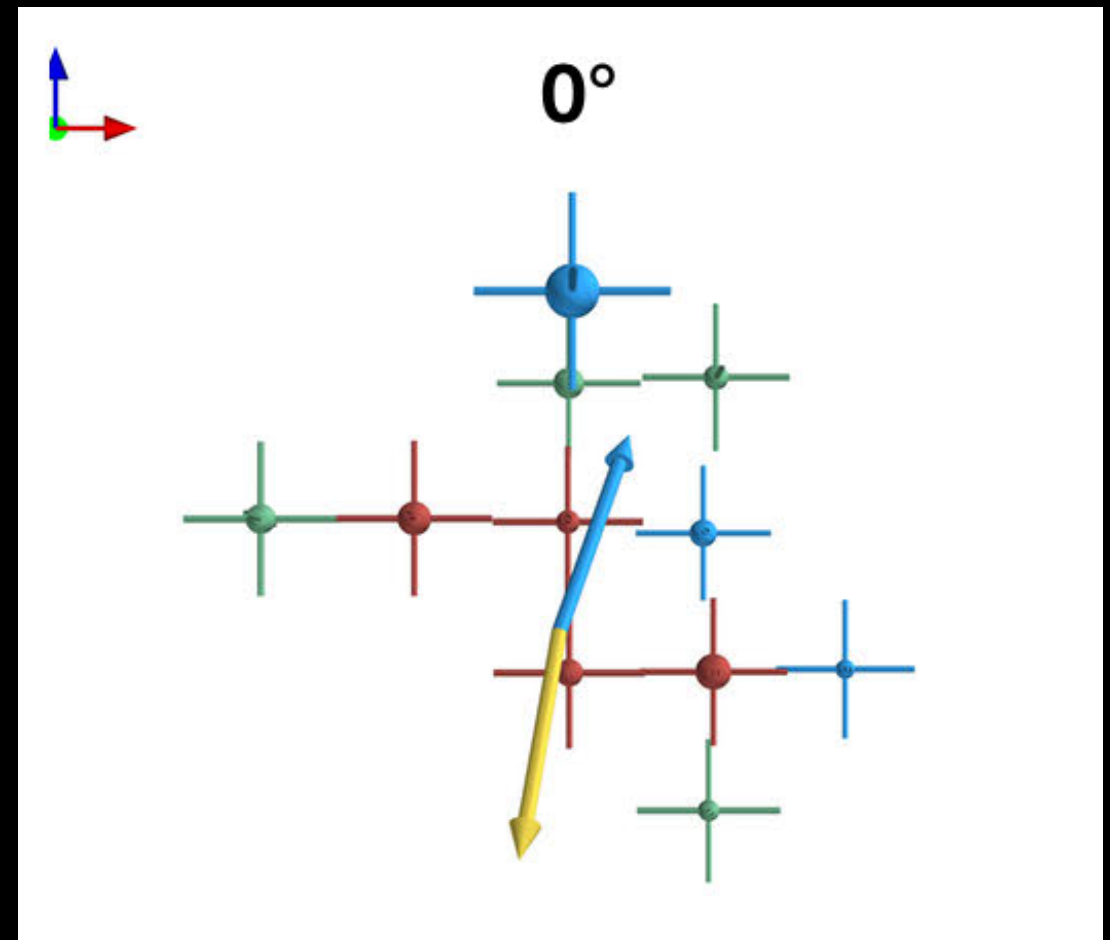
Kinematics of ^{44}Ti line showed that Ti is opposite to NS motion

Blue arrow: direction of Ti

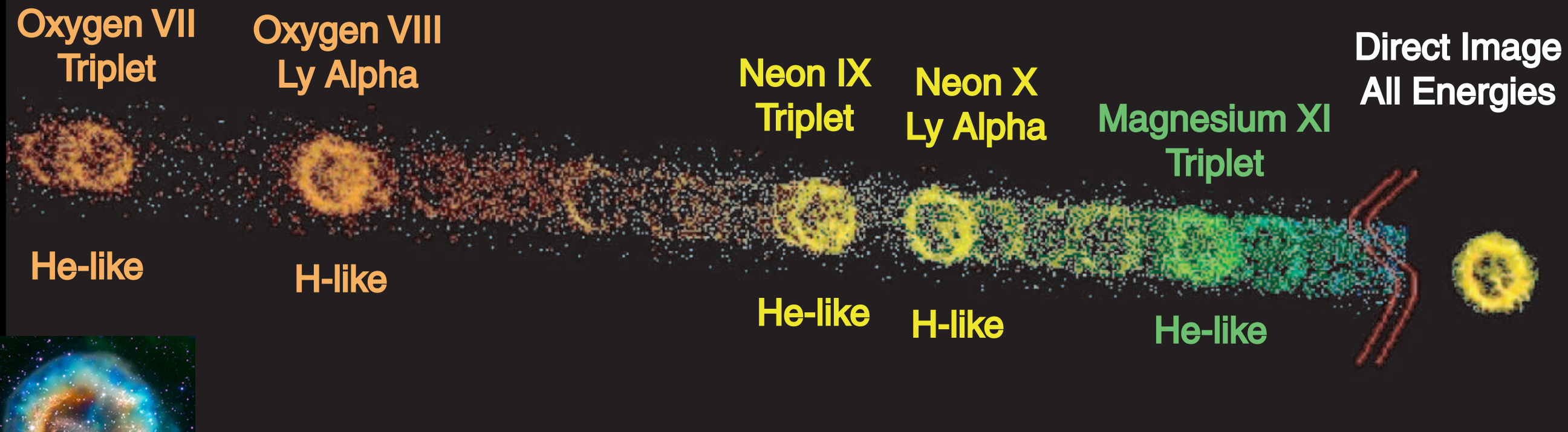
Yellow arrow: direction of NS



Grefenstette et al. 2017

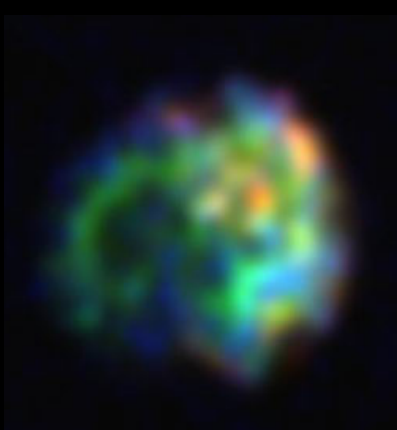
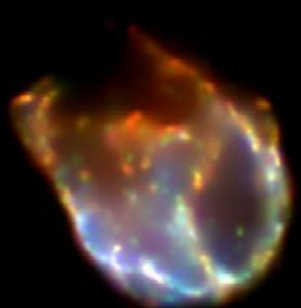


Limitations of Gratings



SNR 1E 0102.2-7219

Flanagan et al. 2004

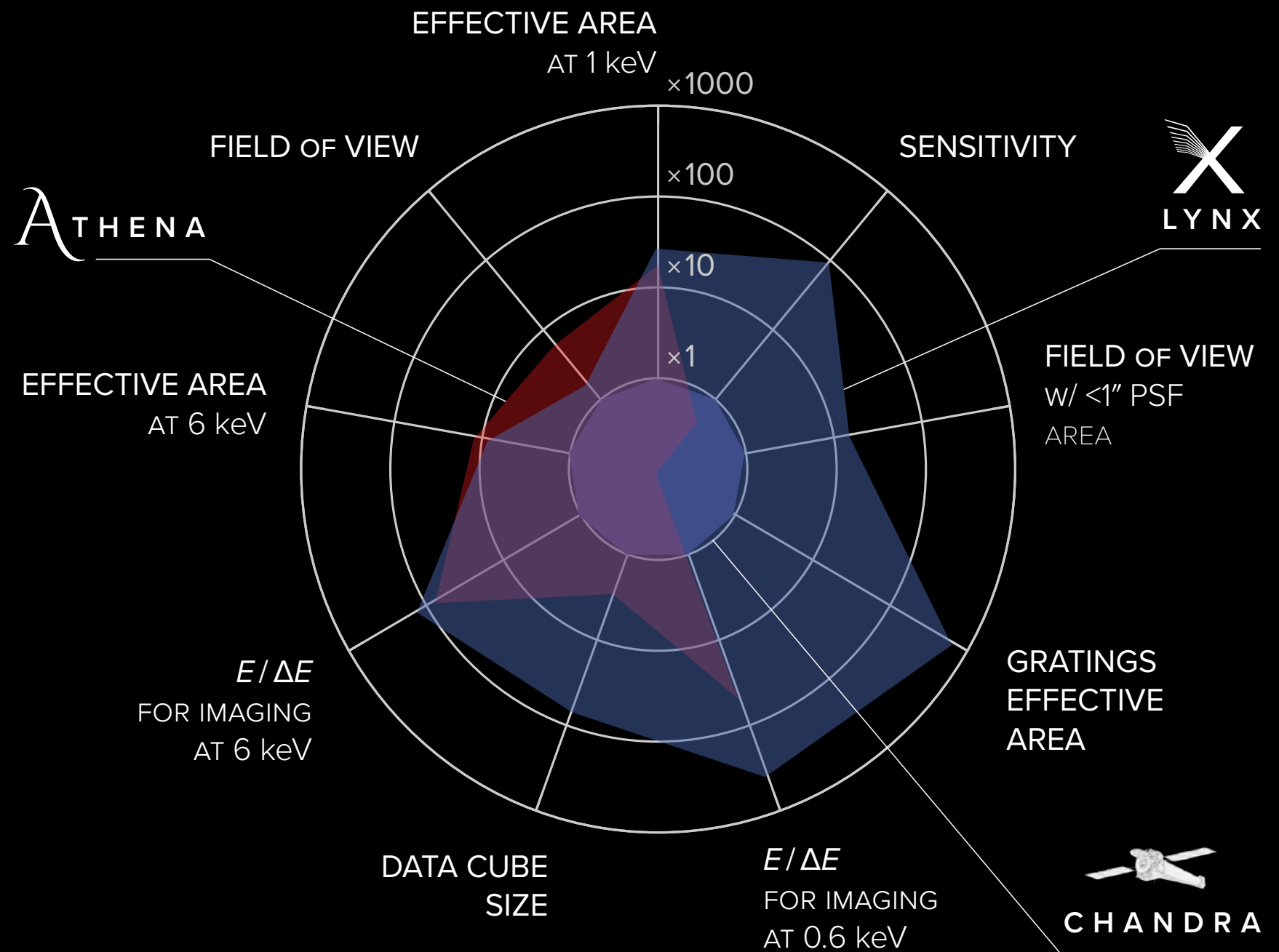


Dewey 2002

Future: Microcalorimeters

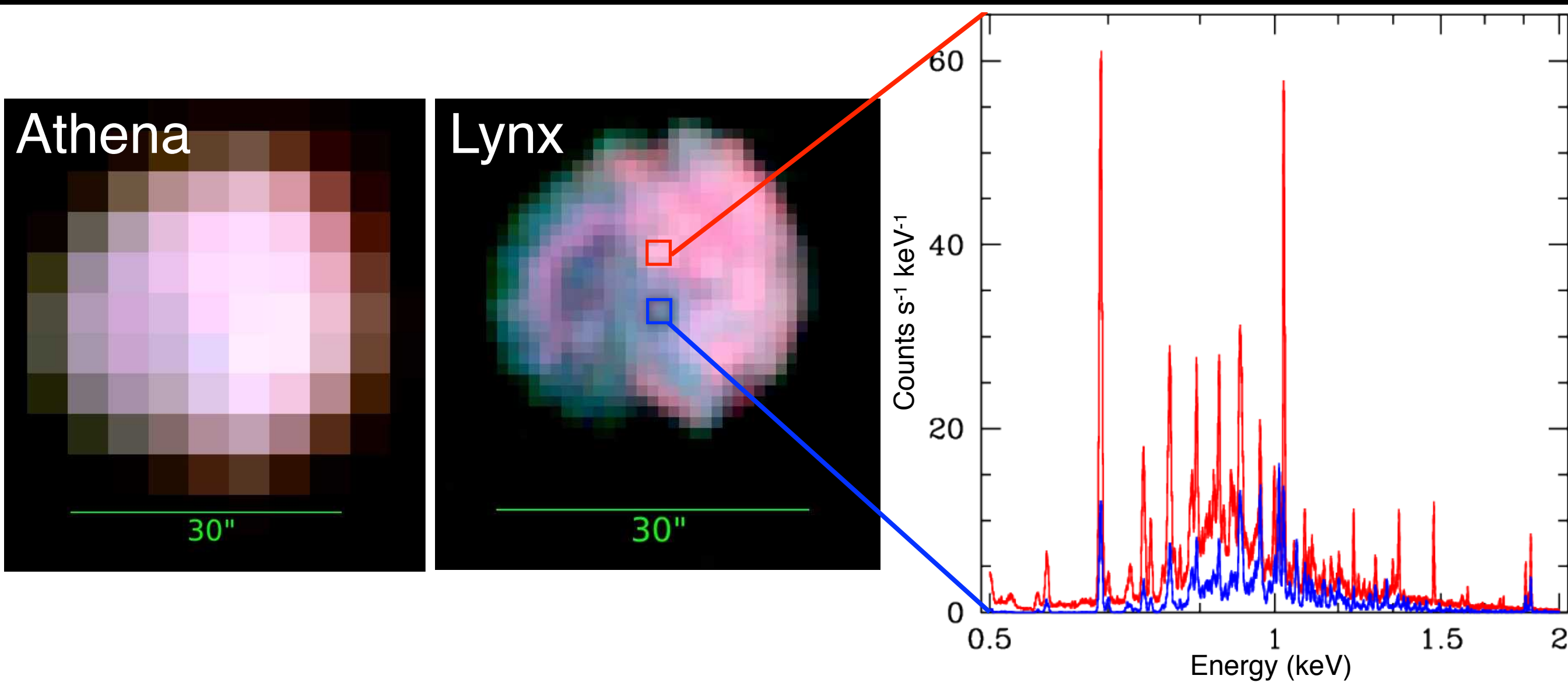
Microcalorimeters on XRISM, Athena, and Lynx are going to revolutionize SNR science, giving a 3D view of ejecta

Lynx is successor mission to Chandra (30x effective area); will have 1" pixel microcalorimeter



Future: Lynx

1" pixels on microcalorimeter reduces confusion between different spectral components to enable precise measures of velocities, ejecta mixing, plasma properties



Lopez et al. 2019, arXiv: 1903.09677

Conclusions

SNR morphologies in different wavebands reflect the explosion asymmetries, the inhomogeneous environments, and the ambient magnetic field/particle acceleration properties

Type Ia SNRs are more circular and symmetric in X-rays and IR, reflecting their distinct explosions & environments.

In radio, morphology reflects ambient density and B-field. Radio morphology becomes increasingly asymmetric with age due to expansion into inhomogeneous medium.

Distinct morphologies of different elements useful to constrain explosion/progenitors and origin of neutron star kicks

3D maps of SNRs are even more powerful at revealing asymmetries, microcalorimeters will revolutionize field